# ULF wave identification in the magnetosheath: The k-filtering technique applied to Cluster II data

F. Sahraoui, Jean-Louis Pinçon, G. Belmont, L. Rezeau, N. Cornilleau-Wehrlin, P. Robert, L. Mellul, J. M. Bosqued, A. Balogh, P. Canu, et al.

JOURNAL OF GEOPHYSICAL RESEARCH, VOL. 108, NO. A9, 1335, doi:10.1029/2002JA009587, 2003

***Correction published 24 April 2004***

# ULF wave identification in the magnetosheath: The k-filtering technique applied to Cluster II data

F. Sahraoui,[1] J. L. Pinçon,[3] G. Belmont,[1] L. Rezeau,[1,2] N. Cornilleau-Wehrlin,[1] P. Robert,[1] L. Mellul,[1] J. M. Bosqued,[5] A. Balogh,[4] P. Canu,[1] and G. Chanteur[1]

Received 16 July 2002; revised 18 March 2003; accepted 14 May 2003; published 5 September 2003.

[1] The magnetic fluctuations in the magnetosheath are studied, thanks to Cluster II data. The k-filtering technique is applied to explore ULF magnetic fluctuations using STAFF (Spatio-Temporal Analysis of a Field Fluctuations) data. Based on multipoint measurements, the k-filtering technique allows, for the first time, to estimate the Magnetic Field Energy Distribution (MFED) in both the angular frequency and wave vector space. We show how the localisation of the magnetic energy in the ($\omega$, **k**) domain can be used to identify the linear modes that can propagate in the magnetosheath. A comparison between k-filtering results and prediction of the linear theory is performed. For the frequencies examined the magnetic energy seems to be distributed over the low frequency modes: mirror, Alfvén, and slow modes. Estimation of Doppler shift shows that each frequency observed is the superposition of different frequencies in the plasma frame. This ''mixture of modes'' at a given observed frequency explains why the fluctuations are generally not observed to be polarized, as shown in previous studies. Some other implications on a weak turbulence approach of the magnetic fluctuations in the magnetosheath are discussed. *INDEX TERMS:* 2728 Magnetospheric Physics: Magnetosheath; 7819 Space Plasma Physics: Experimental and mathematical techniques; 2149 Interplanetary Physics: MHD waves and turbulence; 6984 Radio Science: Waves in plasma; 2772 Magnetospheric Physics: Plasma waves and instabilities; *KEYWORDS:* terrestrial magnetosheath, magnetic turbulence, Cluster mission, STAFF data k-filtering technique, ULF modes

**Citation:** Sahraoui, F., et al., ULF wave identification in the magnetosheath: The k-filtering technique applied to Cluster II data, *J. Geophys. Res.*, *108*(A9), 1335, doi:10.1029/2002JA009587, 2003.

## 1. Introduction

[2] The magnetic fluctuations in the magnetosheath and in the surrounding regions have been, for many years, a subject of both theoretical and experimental researches [*Tsurutani et al.*, 1982; *Luhmann et al.*, 1986; *Song et al.*, 1992; *Anderson and Fuselier*, 1993; *Gary et al.*, 1993; *Hubert et al.*, 1998; *Rezeau et al.*, 1999; *Hubert*, 1994]. Many of the experimental studies on the waves in the magnetosheath, which is commonly imaged as a turbulent region, have been dedicated to linear mode identification focusing on the low frequency range [0, $\sim f_{ci}$], $f_{ci}$ being the proton gyro-frequency, [*Anderson et al.*, 1994; *Denton et al.*, 1994; *Lacombe et al.*, 1992, 1995; *Song et al.*, 1994; *Lucek et al.*, 1999]. In the absence of multisatellite missions the identification of the waves could not be based on anything but the ''wave polarization'', i.e., analyzing the relationship existing between the different components of the electromagnetic field and the plasma characteristics. Therefore almost all these works were realized by comparing of a set of physical experimental parameters (c.f. the so-called ''transport ratios'') to the corresponding theoretical ones, such as the perpendicular and parallel components (with respect to the background magnetic field $\mathbf{B}_o$) of the magnetic fluctuations, the correlation between the phases of the parallel magnetic pressure and the thermal pressure, polarization and propagation direction of the fluctuations. These analyses have been done successfully over data intervals of few minutes to few hours in different regions of the magnetosheath: the vicinity of the magnetopause, the middle of the magnetosheath, the downstream bow-shock. It is worth noticing that these methods have been applied most generally when the fluctuations are ''wave-like'', i.e., with a clear spectral peak, rather than ''turbulent-like'' (e.g., with power-law continuous spectra). They have allowed the authors to identify the dominant mode component of the waves for a given time interval (in relation, when possible, with the fastest growing instability). Roughly speaking, the mentioned studies concluded to the identification of Alfvén-like or ion cyclotron waves when the transverse component was dominant and the mirror-like or slow waves when the

[1]Centre d'etude des Environnement Terrestre et Planétaires/Centre National de la Recherche Scientifique/Institut Pierre Simon Laplace, Vélizy, France.
[2]Also at Université Pierre et Marie Curie, Paris, France.
[3]Laboratoire de Physique et de Chimie de l'Environnement, Orléans, France.
[4]Space and Atmospheric Group, The Blackett Laboratory, Imperial College, London, UK.
[5]Centre d'Etude Spatiale des Rayonnements, Toulouse, France.


0148-0227/03/2002JA009587

fluctuations were compressional [*Song et al.*, 1992]. Moreover, the nature of the identified linear waves seems to be different, depending at once on the depth in the magnetosheath, the geometry of the shock, the plasma beta, the ion temperature anisotropy and the frequency range analyzed: high plasma beta with small ion temperature anisotropy (e.g., $\beta_{i\|} \approx 2$ and $A_i = T_\perp/T_\| - 1 \approx 0.4$) seems to be favorable to mirror modes, whereas low beta and large ion temperature anisotropy (e.g., $\beta_{i\|} \approx 0.2$ and $A_i \approx 2$) favor EMIC (ElectroMagnetic Ion Cyclotron) waves [*Anderson et al.*, 1994]. *Song et al.* [1994] have shown that (1) Alfvén waves seem to be dominant in the frequency range [1, 100] mHz near the quasi-perpendicular bow shock (the ion gyrofrequency was around 0.5 Hz); (2) in the inner and the middle of the magnetosheath the alfvenic fluctuations are below 10 mHz, the fast mode occurring for higher frequency (~80 mHz); and (3) the slow/mirror modes occur in the inner/middle magnetosheath at intermediate frequencies. *Hubert et al.* [1998], have noted that the nature (mirror or alfvenic) of the waves depends upon the depth in the magnetosheath more than upon the local physical parameters of the plasma.

[3] Beyond this set of well-established results, it appeared very difficult to go further from monosatellite data: all these analyses have indeed serious limitations, which have to be pointed out. *Denton et al.* [1995] have outlined the difficulty, for some events, to identify any linear mode; they suggested that multiple modes are superimposed in the same frequency range or that nonlinear effects are at work, which may yield to the loss of the linear properties. They have also drawn attention on the difficulty of distinguishing the ion cyclotron from the mirror waves for the propagation direction where the two modes degenerate. Another basic ambiguity was mentioned by *Gleaves and Southwood* [1991] for distinguishing between mirror and slow modes, since they are both compressional with an anticorrelation between their magnetic parallel component and the density fluctuations (they are 180° out of phase). Except for *Song et al.* [1994], who tried to find a new criterion for performing this distinction, most of the analyses have identified as a mirror wave any compressional wave with an anticorrelation between thermal and magnetic pressure, with the argument that slow waves should be strongly damped by kinetic effects. It is worth noticing that under this form the argument holds for a low beta plasma but that it can be generalized: the Landau damping actually concerns the mode that has a parallel phase velocity close to the thermal velocity, which is indeed the slow mode when beta is small but which is the fast mode whenever beta is larger than unity. The ambiguity between the two compressive waves may also be related to the MIAOW (mirror and slow) waves mentioned by *Omidi and Winske* [1995] (see section 5) and have been previously identified in the magnetosheath by *Balikhin et al.* [2001].

[4] An additional limit arises when trying to determine the propagation direction of the identified waves. In all the mentioned studies, for the reason of the number of independent parameters measured in monosatellite missions, the uniqueness of the wave vector had to be assumed for each given frequency (with a direction determined for instance by Minimum Variance Analysis). This restriction to monochromatic plane waves (one **k** for one frequency), even when justified, can only provide information on the mode that supports the dominant part of the energy. It therefore causes a loss of information on any other weak component(s), which can compromise any further analysis, concerning in particular the polarization. When the energy does indeed propagate on several plane waves (i.e., with several wave vectors) with comparable energies, any study assuming the uniqueness of the wave vector should be a failure. The last point to be noticed is that in the magnetosheath all the characteristic velocities have the same order of magnitude, which gives an important role to the Doppler effect: one has always to keep in mind that the observed waves are measured in the spacecraft frame while the theoretical linear waves are derived in the plasma frame [*Omidi et al.*, 1994; *Song et al.*, 1994].

[5] Before the Cluster-II mission, experimental analysis elaborated to understand the physics of the magnetosheath have suffered from the spatiotemporal ambiguity that characterizes the one-satellite measurements and sometimes also from the lack of simultaneous field and plasma data. In fact, missions with two satellites have already allowed to distinguish the temporal variation of the fluctuations from the spatial ones but only in general, along the direction between the two satellites [*Gleaves and Southwood*, 1991]. *Dudok de Wit et al.* [1995] have shown how one can extrapolate from the dispersion relation $\omega(k_d)$, where $k_d$ is the component of **k** along the direction between the two satellites, to a dispersion relation $\omega(k)$, where $k$ is the modulus of **k**, when a minimum variance analysis can be used (assuming a plane wave) or when some statistical assumptions can be made on the **k** directions in presence [see also *Balikhin et al.*, 1997; *Bates et al.*, 2001]. Now, thanks to Cluster II data, it becomes potentially possible to remove entirely this ambiguity and hence to explore three-dimensional (3-D) motions of the electromagnetic/particle structures from four point measurements. In the analysis below, magnetic data are provided by the STAFF experiment which is devoted to study magnetic fluctuations ranging from 0 to 4 kHz [*Cornilleau-Wehrlin et al.*, 1997], FGM (Flux Gate Magnetometer) experiment [*Balogh et al.*, 1997] provides the static magnetic field $\mathbf{B}_o$, ion velocities and temperatures data are obtained thanks to CIS (Cluster Ion Spectrometer) experiment [*Rème et al.*, 1997], and the electron density is provided by WHISPER (Waves of High frequency and Sounder for Probing of Electron density by Relaxation) experiment [*Décréau et al.*, 1997].

[6] In the present study we focus on the ULF (Ultra Low Frequency, ~few Hz) magnetic fluctuations in the magnetosheath. From a complete data set from Cluster II mission we use the tools that allow the most refined analysis; we show that 3-D exploration of the magnetic fluctuations reveals a complex physics, involving more than one plane wave for each observed frequency. To our knowledge, this is the first time that linear mode identification in the magnetosheath can be done from the direct comparison between the theoretical dispersion relations and a 3-D experimental determination. Other aspects are finally briefly evoked, such as the importance of Doppler shift on the polarization analysis and the weak nonlinear coupling of waves in the magnetosheath. This new knowledge of the ULF magnetic fluctuations in the magnetosheath will bring significant information to constrain the models of reconnection and

transfers at the magnetopause, such as *Belmont and Rezeau* [2001].

## 2. The k-Filtering Technique

[7] Multisatellite measurements like those performed on board Cluster open fundamental new possibilities to identify and to characterize spatial plasma structures. The k-filtering technique is a generalized minimum variance technique introduced into the field of space science by *Pinçon and Lefeuvre* [1991]. Assuming the wave-field is time stationary and homogeneous in space, it allows to obtain optimum estimates of the power spectra density, in the frequency-wave vector space from multipoint data measurements recorded simultaneously at a few points in space. In the present study we apply this technique to three data sets, which are the three components of the magnetic field fluctuations $\mathbf{B}(\mathbf{r}, t)$, as recorded on board the four Cluster spacecraft by the STAFF experiment.

[8] Let $\mathbf{B}(\mathbf{r}_\alpha, t)$ ($\alpha \in \{1, 2, 3, 4\}$) be the magnetic field fluctuation vectors recorded at the four Cluster spacecraft positions $\mathbf{r}_\alpha$. The correlation matrix for two measurements is of particular importance for the characterisation of the field. It is constructed as the dyadic product of two measurement vectors $\mathbf{B}(\mathbf{r}_\alpha, t + \tau)$ and $\mathbf{B}(\mathbf{r}_\beta, t)$. It is written

$$\mathbf{M}(t+\tau, \mathbf{r}_\alpha, t, \mathbf{r}_\beta) = \langle \mathbf{B}(t+\tau, \mathbf{r}_\alpha)\mathbf{B}^*(t, \mathbf{r}_\beta)\rangle \quad (1)$$

where the asterisk means transpose and complex conjugation and $\langle\ \rangle$ denotes an ensemble average over a large number of data set, which is replaced here by a time average using the ergodic hypothesis. Assuming the wave field is stationary and homogeneous means that all its statistical properties are invariant to a shift of the time origin and to a translation of the space origin. Strict conditions for time stationary and homogeneity cannot be met in space, particularly at the vicinity of geophysical boundaries such as the magnetopause or the bow shock. Fortunately, the data used in the k-filtering technique are the space-time correlation matrices, and to provide reasonable data statistics, statements of "weak" time stationarity and space homogeneity are sufficient: the wave-field has only to be time stationary during time intervals longer than the longer period studied in the wave-field and to be translation invariant over distances larger than the maximum wavelength studied in the field.

[9] In such a case the correlation matrix depends only on $\tau$ and $\mathbf{r}_{\alpha\beta}$ (with $\mathbf{r}_{\alpha\beta} = \mathbf{r}_\alpha - \mathbf{r}_\beta$)

$$\mathbf{M}(t+\tau, \mathbf{r}_\alpha, t, \mathbf{r}_\beta) = \mathbf{M}(\tau, \mathbf{r}_{\alpha\beta}). \quad (2)$$

[10] A frequency representation of the magnetic field fluctuations is obtained by performing a temporal Fourier transform of $B_x(\mathbf{r}_\alpha, t)$, $B_y(\mathbf{r}_\alpha, t)$, and $B_z(\mathbf{r}_\alpha, t)$. The correlation matrix element in the frequency domain for a pair of measurements is then given by

$$\mathbf{M}(\omega, \mathbf{r}_{\alpha\beta}) = \langle \mathbf{B}(\omega, \mathbf{r}_\alpha)\mathbf{B}^*(\omega, \mathbf{r}_\beta)\rangle. \quad (3)$$

[11] A relationship between the measured correlation matrix $\mathbf{M}(\omega, \mathbf{r}_{\alpha,\beta})$ and a representation of the wave-field in the $(\omega, \mathbf{k})$ domain can be expressed through a Fourier transform in $\mathbf{k}$-space, we have

$$\mathbf{M}(\omega, \mathbf{r}_{\alpha\beta}) = \int_k \mathbf{P}(\omega, \mathbf{k}) e^{-i\mathbf{k}\cdot\mathbf{r}_{\alpha\beta}} d\mathbf{k} \quad (4)$$

where $\mathbf{P}(\omega, \mathbf{k})$ is the spectral wave-field energy density matrix which trace, noted $P(\omega, \mathbf{k})$, is the magnetic wave-field energy density distribution in the frequency wave-vector domain. Owing to the limited number of vectors $\mathbf{r}_{\alpha\beta}$ for which $\mathbf{M}(\omega, \mathbf{r}_{\alpha\beta})$ can be estimated in the frame of Cluster, determining $P(\omega, \mathbf{k})$ by the use of a linear method for inverting equation (4) is of no interest. To obtain an acceptable resolution in the k-domain, a specific method called k-filtering was developed. It is a generalization to a vector signal measured in space of the method, originally developed by *Capon* [1969] for estimating the frequency wave number spectrum associated with seismic waves measured on the ground at several points.

[12] The k-filtering technique allows us to obtain an optimal estimation of $P(\omega, \mathbf{k})$ from the knowledge of the matrices $\mathbf{M}(\omega, \mathbf{r}_{\alpha\beta})$. We adopt a filter-bank approach to obtain the spectral energy density estimator. Each filter is related to a different $(\omega, \mathbf{k})$ pair and is built in such a way that only the energy associated with the angular frequency $\omega$ and the wave vector $\mathbf{k}$ is extracted from the data. It can be shown [*Pinçon and Motschmann*, 1998] that the problem of the filter determination can be solved using the Lagrange multiplier technique. The details of the calculation are beyond the scope of this work. For a complete exposition the reader is referred to *Pinçon and Lefeuvre* [1991] and *Pinçon and Motschmann* [1998]. The final expression for the $P(\omega, \mathbf{k})$ estimation is given by

$$P(\omega, \mathbf{k}) = Tr\left\{ \left[\mathbf{H}^*(\mathbf{k})\mathbf{M}^{-1}(\omega)\mathbf{H}(\mathbf{k})\right]^{-1} \right\}, \quad (5)$$

with $\mathbf{H}(\mathbf{k})$ is the matrix defined as follows

$$\mathbf{H}(\mathbf{k}) = \begin{bmatrix} \mathbf{I}\exp(-i\mathbf{k}\cdot\mathbf{r}_1) \\ \mathbf{I}\exp(-i\mathbf{k}\cdot\mathbf{r}_2) \\ \mathbf{I}\exp(-i\mathbf{k}\cdot\mathbf{r}_3) \\ \mathbf{I}\exp(-i\mathbf{k}\cdot\mathbf{r}_4) \end{bmatrix}. \quad (6)$$

[13] $\mathbf{I}$ is the $(3 \times 3)$ unit matrix and thus $\mathbf{H}(\mathbf{k})$ is a $(12 \times 3)$ matrix. This matrix contains the information about the Cluster configuration in space. The $\mathbf{M}(\omega)$ matrix is a $(12 \times 12)$ matrix which contains all the correlation matrices $\mathbf{M}(\omega, \mathbf{r}_{\alpha\beta})$ that can be estimated from the four Cluster spacecraft. If no a priori information is available, the expression given by equation (5) is an optimum estimator of the wave-field spectral energy density. If some information on the data is available, such as an external constraint that could be imposed by physical consideration, one may improve the quality of the final estimator by including it during the process of the filter design. The various solutions presented in this paper were obtained from an estimator which take into account the constraint $\nabla \cdot \mathbf{B} = 0$.

[14] The practical interest of the $P(\omega, \mathbf{k})$ estimator is heavily related to its sensitivity to the propagation of the statistical errors in the data. To ensure the validity of the

obtained solutions, one has to be sure that a small fluctuation of the measured data set will give a reasonably small modification of the obtained solution. From this point of view the quality of the solution provided by the k-filtering estimator is characterised by two quantities: the $P(\omega, \mathbf{k})$ bias errors, $\langle \delta P \rangle$, and its stability, $\langle \delta P^2 \rangle / P^2$. Both quantities have been studied in detail by *Pinçon and Lefeuvre* [1991]. This study has shown that the $P(\omega, \mathbf{k})$ estimator is unbiased if the elements of the $\mathbf{M}(\omega)$ matrices are unbiased. Such a condition is fulfilled when the frequency power spectra are smooth. It has also been shown that the stability of the $P(\omega, \mathbf{k})$ estimator is equal to the stability of the data, multiplied by a factor that depends on the number of measuring points, on their geometry, and on the data itself. An exact calculation of this multiplying factor can be made in the special case of a wave-field consisting of an electromagnetic plane wave embedded in noise. In such a case the multiplying factor is equal to 1 whatever the number of measuring points and their geometry. In the analysis of real data, generally, one cannot derive an analytical expression for the stability. However, the results obtained in the analysis of plane wave may be used as guidelines. They tell us that the crucial point is the conditioning of the $\mathbf{M}(\omega)$ matrix. In a practical sense, to make a first appraisal of the stability in the solution, it will be always possible to compare solutions that were obtained after adding random noise to the data at levels comparable with the errors in these data. Slight modifications of the solutions will indicate that the solution is stable.

[15] As discussed above, the reliability of the frequency wave-vector spectra provided by the spectral energy density estimator is likely to be sensitive to the quality of the initial temporal Fourier transform. In the present study, for a given time interval $T$, instead of calculating the FFT over consecutive equal time subintervals $T_0$ ($T_0 = 41$ s), we compute it by using a sliding window over sets of 1024 points sampled at $\delta t = 0.04$ s, which leads to the sampling frequency $\delta f \approx 0.024$ Hz. This allows to deal with a smooth spectrum resulting by averaging over the whole number of FFTs. Furthermore, to avoid any inaccuracy in the phase determination due to boundary effect [*Rezeau et al.*, 1999], each data segment corresponding to a time interval of length $T_0$ is multiplied by a $\cos^3(t)$ window function before computing the FFTs.

[16] The question of the accuracy of the k-filtering technique is discussed in section 5. Let us just recall that applications to synthetical data have demonstrated the ability of the method to determine the $P(\omega, \mathbf{k})$ for wave-fields corresponding to linear combination of incoherent magneto-ionic modes [*Pinçon and Lefeuvre*, 1992]. The resolving power depends on the number of satellites, on their geometry and on the level of the ambient noise for each satellite.

[17] The main precaution to be taken when using the k-filtering technique concerns the so-called "spatial aliasing" effect. Actually, it is not an effect coming from the k-filtering technique itself but an inevitable consequence of the four spacecraft configuration of Cluster. This effect is comparable to the more well-known "frequency aliasing" effect, but contrary to this one, which can be avoided by low-pass filtering before sampling, the spatial aliasing is unavoidable because the field is essentially sampled at the points of the four spacecraft and cannot be recorded continuously in space. The origin of the spatial aliasing comes from the fact that a fleet of four spacecraft like Cluster does not allow to distinguish two plane waves having the same frequency when their wave vectors $\mathbf{k}$ and $\mathbf{k} + \Delta\mathbf{k}$ differ by a vector $\Delta\mathbf{k}$. The $\Delta\mathbf{k}$ belongs to an infinite set of vectors defined by

$$\Delta\, \mathbf{k} \cdot \mathbf{r}_\alpha = 2\pi m_\alpha + \varphi \qquad \forall \alpha \in \{1, 2, 3, 4\} \tag{7}$$

where $m_\alpha$ are signed integers. This set is generated by the linear combinations of three basic reciprocal vectors [*Neubauer and Glassmeier*, 1990; *Chanteur*, 1998]:

$$\Delta\mathbf{k} = n_1 \Delta\mathbf{k}_1 + n_2 \Delta\mathbf{k}_2 + n_3 \Delta\mathbf{k}_3,$$

with

$$\begin{aligned} \Delta\mathbf{k}_1 &= (\mathbf{r}_{31} \times \mathbf{r}_{21}) 2\pi / V \\ \Delta\mathbf{k}_2 &= (\mathbf{r}_{41} \times \mathbf{r}_{21}) 2\pi / V \\ \Delta\mathbf{k}_3 &= (\mathbf{r}_{41} \times \mathbf{r}_{31}) 2\pi / V \\ V &= \mathbf{r}_{41} \cdot (\mathbf{r}_{31} \times \mathbf{r}_{21}). \end{aligned} \tag{8}$$

[18] Wave vectors delivered by the k-filtering technique belong to the cell of the reciprocal space spanned by $\mathbf{k} = e_1\, \Delta\mathbf{k}_1 + e_2\, \Delta\mathbf{k}_2 + e_3\, \Delta\mathbf{k}_3$ with $-0.5 < e_i \leq 0.5$ ($i = \{1, 2, 3, 4\}$), which corresponds to the first Brillouin zone in solid state physics. This fundamental cell corresponds roughly to waves having wavelengths larger than the minimum distance between spacecraft. If the most significant part of the wave field energy is associated only with $\mathbf{k}$ vectors within this volume then the $P(\omega, \mathbf{k})$ estimator within this basic cell is free of aliasing and the observed peaks are physically meaningful. If this supposition is not valid, some of the observed peaks may be actually aliased peaks wrapped back into the basic cell. In such a case, to identify whether a given peak is an alias requires additional physical information. The constraint $\nabla \cdot (\mathbf{B}) = 0$ which can be introduced in the k-filtering program provides such information. It will be demonstrated in section 4 that one of the energy peaks evidenced by the k-filtering technique is indeed an alias of physical modes lying outside the fundamental cell, but we will see that the investigation of the frequency variations allows also to spot, and possibly to solve, the difficulty.

[19] The validity of the spectral energy density estimator is also limited by the shape of the actual Cluster configuration in space which geometry may widely vary in shape and size over the orbit. An unambiguous three-dimensional characterization of the wave-field requires that the four Cluster spacecraft be in a good three-dimensional configuration. Consequently, it is necessary to check on the shape of the spacecraft configuration before applying the k-filtering technique. This can be easily done from the knowledge of the tetrahedron geometric factors [*Robert et al.*, 1998].

## 3. The k-Filtering Technique Applied to Cluster II Data

[20] On 18 February 2002 around 0400:00 the satellites were in the magnetosphere, they crossed the magnetopause at 0459:00, and they remained in the magnetosheath till

0748:00, when they crossed the shock. The density, obtained from Whisper experiment, varies from 30 $cm^{-3}$ in the inner magnetosheath close to the magnetopause to about 50 $cm^{-3}$ just downstream of the shock. Data used in the following study were obtained around 0534:00, the spacecraft were in the magnetosheath near the magnetopause (density $n \approx$ 36 $cm^{-3}$). Their positions were close to $X_{gse}$ = 5.6 $R_e$, $Y_{gse}$= 4.6 $R_e$, $Z_{gse}$ = 8.4 $R_e$, and they were separated by about 100 km.

[21] The Cluster configuration associated with this data set was checked to be appropriate for 3-D analysis. Two geometrical factors, elongation $E$ and planarity $P$, are defined as control parameters of the 3-D configuration of the spacecraft: $P = 1$ is related to a "pancake" configuration of the satellites, whereas $E = 1$ reflects a "cigar" configuration; values close to zero of these factors is the ideal 3-D configuration. Intermediate values $P \leq 0.4$ and $E \leq 0.4$ were estimated to be well appropriate to describe a real 3-D configuration [*Robert et al.*, 1998]. In our case we have $P \approx$ 0.1 and $E \approx 0.1$.

[22] The k-filtering technique is applied over a time interval $T$ = 164 s, starting from 0534:1.15 s (Figure 1). The data are filtered using a high-pass filter with a cut-off frequency $f_{\text{cut-off}}$ equal to 0.35 Hz. This filter only intends to avoid any problem with the spacecraft spin, which may pollute the magnetic data at the frequencies close to 0.25 Hz. We checked that modifying the cut-off frequency does not change significantly the results, which exhibit a good stability in this respect: the large scales do not influence the small ones. It is worth noticing that this satisfactory property is not in contradiction with the homogeneity hypothesis; invoking space homogeneity of the small scale fluctuations does not means that the large-scale components are supposed to be absent of the signal, it only means that the small-scale fluctuations are supposed to have the same amplitude at the four points where they are measured.

[23] The modulus of the filtered magnetic fluctuations, normalized to the background magnetic field, is shown in Figure 2 for one satellite. We note that the level of the fluctuations is weaker than 15% of the static magnetic field. As discussed further below, this may be a good argument to support a weak turbulence approach for studying the magnetic fluctuations in the magnetosheath.

[24] The power spectrum of the magnetic fluctuations ranging from 0.35 Hz to 12.5 Hz is presented in Figure 3 (for satellite 1). As noticed in several previous papers [e.g., *Rezeau et al.*, 2001], this spectrum looks like a power-law spectrum, similar to those characterizing the cascade of energy from large to small scales in turbulence theory. In Figure 4 we compare the spectra of the parallel and perpendicular components (with respect to the static magnetic field) of the magnetic fluctuations to the "whole" spectrum (sum of the component spectra). Both components look similar and their levels are quite comparable. Figure 5 shows the different particle data used in the analyses below: the plasma ion velocity, the ion parallel and perpendicular temperatures, and the plasma density. In the following analysis, four different frequencies will be picked up arbitrary in the continuous spectrum (Figure 3). It is worth noticing that these frequencies do not correspond to any spectral peak, i.e., to any "wave-like" phenomenon. The four frequencies analysed below belong to the frequency range $[f_{\text{cut-off}}, f_{\max}]$.

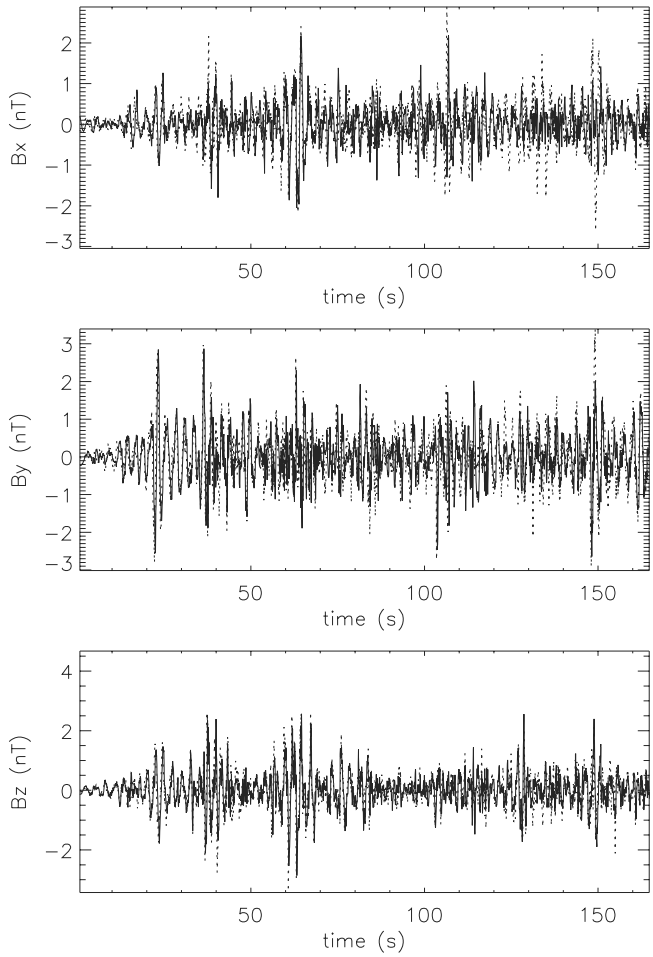


**Figure 1.** STAFF data, 2002/02/18, starting time: 0534:1.15. The studied waveforms data ($T$ = 164 s) filtered at the cut-off frequency $f_{\text{cut-off}}$ = 0.35 Hz are displayed for Cluster 1 (continuous line) and 3 (dotted line). X, Y, Z are the GSE axes.

[25] As it has been explained in section 2, the minimum wavelength that can be calculated by the k-filtering method is determined by the separation between the spacecraft; it can be roughly estimated from $\lambda_{\min} = \frac{2\pi}{k_{\max}} \approx 2d$, where $d$ is a separation between the satellites in a given direction. While looking to k-filtering results in terms of linear waves, this limitation on the measured shortest wavelength turns out to limit the frequency range of the magnetic fluctuations that can be studied. This is due to the existing relationship between frequencies and wave vectors through the phase velocities of the linear waves. Indeed, if we assume the phase velocities of these waves are of the order of the characteristic velocity of the medium $V_{\text{char}}$, the maximum frequency (in the satellite frame) we expect to analyze correctly can be estimated from $f_{\max} \approx \frac{k_{\max}}{2\pi} V_{\text{char}}$.

[26] During the experimental measurements used in this study, Cluster II satellites are separated by distances of about 100 km, which yields to maximum wave vector estimate $k_{\max} \cong 85 \times 10^{-3}$ rd/km. Assuming that $V_{\text{char}} \approx 150$ km/s, the maximum accessible frequency is hence $f_{\max}$ = 2 Hz.

[27] The k-filtering technique allows us to calculate for each frequency, the corresponding 3-D magnetic wave field

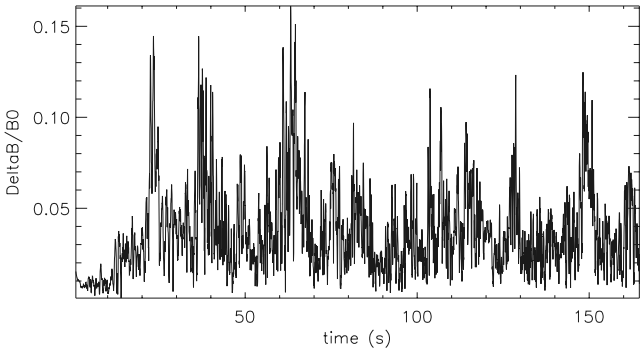


**Figure 2.** Same period as Figure 1. Modulus of the fluctuating magnetic field δB (measured by STAFF on Cluster 1), filtered at the frequency $f_{cut\text{-}off}$ and normalized to the background magnetic field $B_0$.

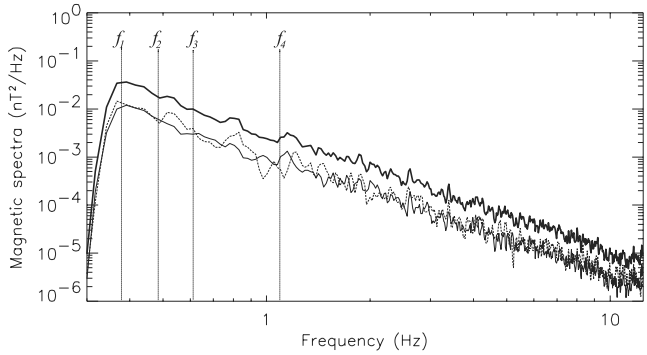


**Figure 4.** Comparison between parallel spectrum $B_{\parallel}^2 = B_z^2$ (dotted line) and the half of the perpendicular one $1/2[B_x^2 + B_y^2]$ (thin line) with the whole spectrum (thick line) for one satellite. Parallel and perpendicular spectra look similar. Vertical lines point the four frequencies studied in the paper.

energy distribution, noted MFED, in the ($k_x$, $k_y$, $k_z$) domain. In the present study we have arbitrary selected four frequencies: $f_1$ = 0.37 Hz, $f_2$ = 0.49 Hz, $f_3$ = 0.61 Hz, and $f_4$ = 1.15 Hz. As an illustration of the information provided by the k-filtering technique, a presentation of the calculated 3-D shape of the MFED associated with frequency $f_1$ is shown in Figure 6. This 3-D view is obtained by displaying the isocontours of the magnetic wave field energy in ($k_x$, $k_y$) plane for 20 different values of $k_z$ ranging from −0.0481 rd/km up to 0.0481 rd/km. Each ($k_x$, $k_y$) plane is restricted to the validity domain defined by $k_x$, $k_y \in [-k_{max}\ ;\ k_{max}]$.

[28] The resolution in **k** space along $k_x$, $k_y$, $k_z$ has been tested to be sufficient to determine the whole MFED without loss of information on its 3-D shape. As can be seen on Figure 6, three regions can be identified, corresponding to three separated maxima with significant energies. They are represented by filled isocontours. Two other secondary peaks (not shown) with a very low energy can also be seen at $k_z = -0.0498$ rd/km. The **k** values for these peaks are reported in Table 1. Once the k-filtering technique is applied to the magnetic field fluctuations, it becomes possible to study how the distribution of the most significant part of the field energy in the (ω, **k**) domain compare with the theoretical dispersion relation of the propagating waves in the magnetosheath. This point is addressed in the following section.

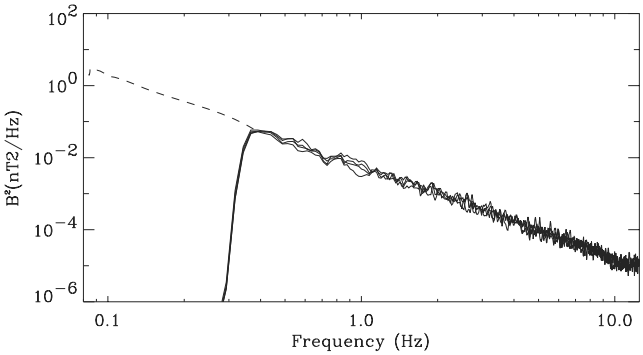


**Figure 3.** Same period as Figure 1. Power spectra of the ULF magnetic fluctuations (measured by STAFF), filtered at the frequency $f_{cut\text{-}off}$ (log scale, on the 4 spacecraft). They are close to a power-law $f^{-\alpha}$ with $\alpha \approx 2.2$.

## 4. Magnetic Energy Distribution and Propagating Linear Modes in the Magnetosheath

[29] As far as we study frequencies of the same order than the ion gyrofrequency in the medium, we suggest to compare the MFED obtained by the k-filtering method in (ω, **k**) domain to linear dispersion relations of the low-frequency modes: mirror, Alfvén, fast, and slow magnetosonic modes. The mirror mode can be added simply by considering it as a nonpropagating mode, i.e., $\omega_{mirror} = 0$ in the plasma frame. The theoretical dispersion relations have been obtained directly as the kinetic solutions provided by the WHAMP program [*Rönnmark*, 1982]. For the sake of simplicity when drawing the plots we sometimes used also different fluid approximations, but the choice of the polytropic indexes is always controlled by the WHAMP solutions.

[30] For an appropriate comparison between the theoretical dispersion relations and the experimental ones, it is useful to define a Magnetic Field-Aligned (MFA) referential, where $z$-axis is along the mean magnetic field $\mathbf{B}_o = B_o\mathbf{z}$, the $x$-axis is perpendicular to $z$-axis in the plane containing the Sun-satellite line and the $z$-axis and is directed towards the Sun, and the y-axis completes the right-handed coordinate system. This is done using the averaged values of the magnetic field components provided by FGM: $B_x(GSE) \approx 5.4$ nT, $B_y(GSE) \approx -20.2$ nT, $B_z(GSE) \approx 1.2$ nT (averaged over data time interval and over the four satellites).

[31] Hereafter, are given the values of the magnetosheath plasma parameters as measured by WHISPER and CIS experiments (Figure 5): plasma density is $n \approx 36$ cm$^{-3}$ and ion temperature is $T_{i\parallel} \approx 140$ eV, $T_{i\perp} \approx 170$ eV, from which we calculate the following parameters that are used in the analysis below: Alfvén velocity is $V_A \approx 78$ km/s, ion gyrofrequency is $f_{ci} \approx 0.33$ Hz, ion Larmor radius is $\rho \approx 79$ km, and ion anisotropy parameter is $A_i \approx 0.22$.

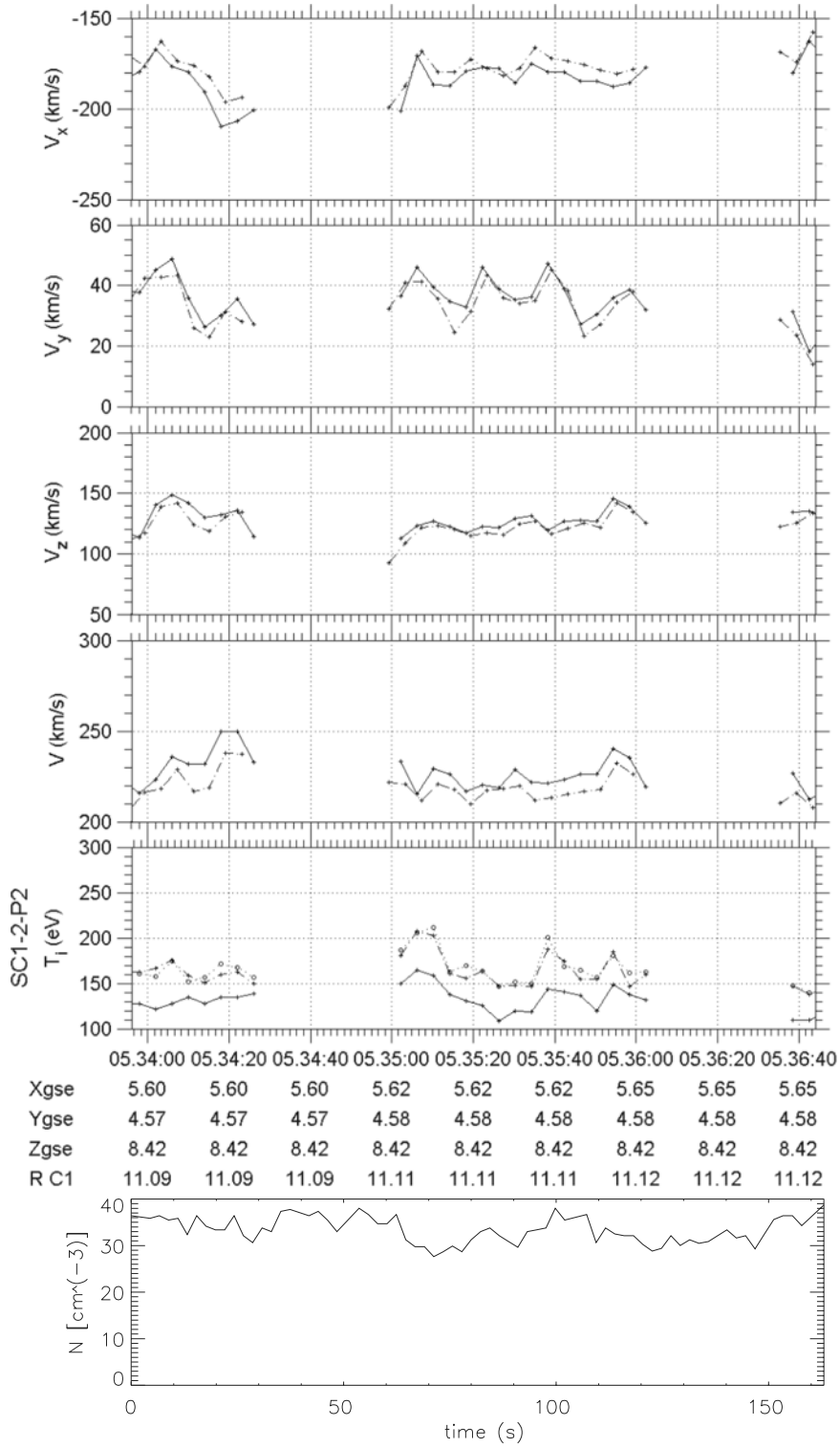


**Figure 5.** Plasma data from CIS2 and Whisper experiments. The four top panels show the onboard plasma velocities from Cluster 1 (continuous line) and 3 (dashed line) in the GSE frame. The fifth panel shows the proton temperatures in the MFA frame (||continuous line, $\perp$1 dashed line, $\perp$2 dashed line). The lowest panel shows the density profile for Cluster 1 (Whisper experiment).

[32] The beta parameters ($\beta_\alpha = 2\mu_o nkT_\alpha/B^2$) are much larger than unity and mainly due to ions. For the ions we can estimate $\beta_{||i} \cong 4.5$, $\beta_{\perp i} \cong 5.4$; for the electrons the PEACE data are not available for the period under study, but the temperature is known to be typically of the order of 40 eV; the electron pressure is therefore very likely to have a negligible role in the wave physics, at least in a first approximation.

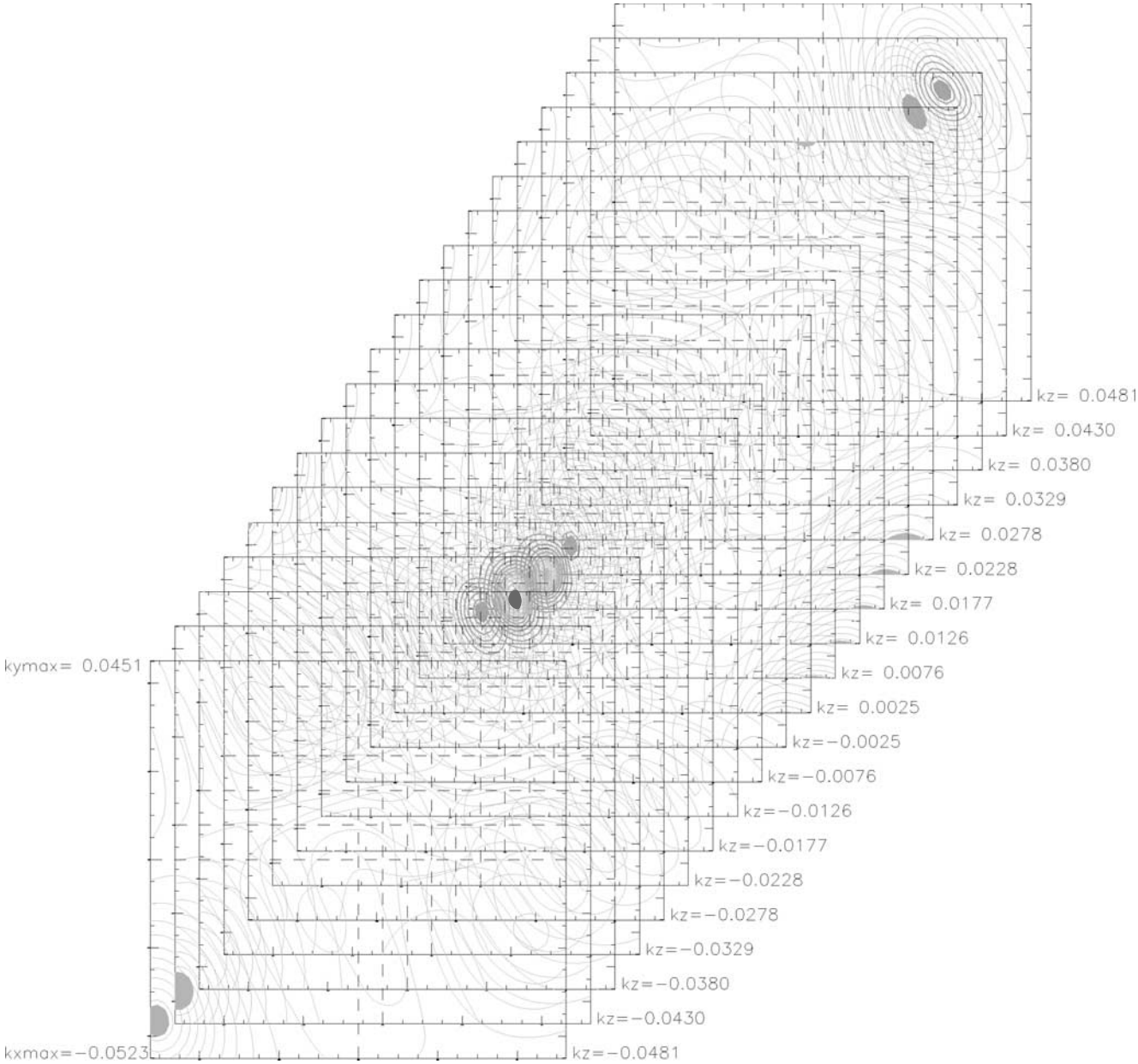


**Figure 6.** Three-dimensional display of the MFED in ($k_x$, $k_y$, $k_z$) space for the frequency $f_1$ = 0.37 Hz. Energy isocontours are drawn in ($k_x$, $k_y$) planes for 20 values of $k_z$ . $k_x$ and $k_y$ values belong respectively to [−0.0523,0.0523] rd/km and to [0.045,0.0451] rd/km. Filled regions represent the three significant maxima. The colour scale goes from black to white with decreasing energy (or from red to blue on the color plate). See color version of this figure at back of this issue.

[33] We will use these values in order to compare the experimental results provided by the k-filtering technique to the classical linear modes in k-space. This first comparison should be considered as an illustration: we are not able, up to now, to provide realistic error bars on all these determinations, neither are we able to estimate the effects of these uncertainties on the final results. One may remind for instance that the particle results (CIS) always derive from a difficult task of calibration and that they come however from detectors with about 20° width each. The values for the flow velocity components given above are obtained by averaging over the spacecraft.

[34] The theoretical dispersion relations and the MFED are computed in the MFA frame defined above. This MFA frame is obviously at rest with respect to the satellite. Because the theoretical results are naturally obtained in the plasma frame, one has to take into account the Doppler effect while comparing theory and data analysis. The Doppler shift can easily be estimated for each **k** value of the result, since the relative velocity between the plasma and the spacecraft is known. This velocity ($V_x \approx -180$ km/s, $V_y \approx -130$ km/s, $V_z \approx -30$ km/s in MFA frame) is derived from the ion velocities provided by the CIS experiment [*Rème et al.*, 1997]. Once estimated, the Doppler shift is used to put

**Table 1.** Doppler Shift is Estimated for Each Maximum of Energy From the Values of the Corresponding Wave Vectors and the Plasma Velocity[a]

| $f_{sat}$, Hz | $(k_x, k_y, k_z) \times 10^{-4}$, rd/km | Energy Density, $nT^2/Hz(rd/km)^3$ | $\theta = (\mathbf{k}, \mathbf{B_0})$ | $\mathbf{k}.\mathbf{v}/2\pi$, Hz | $f_{plasma}$, Hz | Identified Mode |
|---|---|---|---|---|---|---|
| 0.37 | (−97,−53,−59) | 0.0182 | −62° | 0.41 | −0.05 | mirror |
| 0.37 | (292,252,498) → (−98,−38,−102) | 0.00718 | 38° → 46° | −1.57 → 0.40 | 1.94 → −0.40 | mirror (alias → dealiased) |
| 0.37 | (−505,−359,−498) | 0.00272 | −52° | 2.36 | −2.02 | "Alfvén" |
| 0.37 | (−250,340,−498) | 0.00149 | −40° | 0.24 | 0.12 | slow |
| 0.49 | (−115,−53,−76) | 0.00774 | −60° | 0.48 | 0.01 | mirror |
| 0.49 | (310,206,498) → (−80,−84,−102) | 0.00547 | 37° → −49° | −1.53 → 0.45 | 2.02 → 0.04 | mirror (alias → dealiased) |
| 0.49 | (−210,280,−498) | 0.00135 | −36° | 0.26 | 0.22 | slow |
| 0.61 | (−150,−68,−93) | 0.00479 | −61° | 0.60 | 0.01 | mirror |
| 0.61 | (239,236,498) → (−151,−54,−102) | 0.00271 | 35° → −57° | −1.39 → 0.59 | 2.00 → 0.02 | mirror (alias → dealiased) |
| 0.61 | (−280,190,−244) | 0.00200 | −54° | 0.53 | 0.09 | mirror/slow |
| 0.61 | (257,−297,−160) | 0.00147 | −69° | −0.06 | 0.67 | cyclotron |
| 1.15 | (−274,−160,−194) | 0.00076 | −69° | 1.18 | −0.05 | mirror |
| 1.15 | (115,129,397) → (−275,−161,−203) | 0.00065 | 25° → −57° | −0.77 → 1.14 | 1.92 → 0.01 | mirror (alias → dealiased) |
| 1.15 | (−363,7,−295) | 0.00042 | −51° | 1.16 | −0.01 | mirror |

[a]Each peak (in MFA frame) is reported to the corresponding one in the plasma frame.

the theoretical dispersion relations of the low-frequency modes in MFA frame. Under these conditions a realistic comparison between the simplest linear model of propagating waves and the results of k-filtering technique can be done.

[35] The rest of this section is devoted to the study of the relationship between the localisation of MFED maxima and the theoretical dispersion relations of the low frequency modes in the magnetosheath. Thus, for each given frequency ($f_1, f_2, f_3$, and $f_4$), we calculated the dispersion relations of the low-frequency modes in the MFA frame. Then for each frequency the corresponding curves were superimposed to the experimental MFED isocontours. We limited our study to the various ($k_x$, $k_y$) planes containing the most significant maxima of the MFED. The results corresponding to the frequency $f_1$ are presented in Figure 7.

[36] Figure 7 shows that the first maximum (Figure 7a) is localized at $k_z = -0.0059$ rd/km and corresponds to a direction $\theta \approx 62°$ with respect to $\mathbf{B}_o$. This maximum seems to be very close to the $\omega = 0$ line; if the peak is not due to a slow mode (very close itself to the $\omega = 0$ line), it can therefore be identified a priori as a "nonpropagating mode" or a "mirror-like structure," as already reported in several previous papers. For the sake of simplicity we will simply label it as "mirror mode" in the following. However, it must be kept in mind that this cannot be considered a certain identification as long as a more complete analysis, including the polarization for instance, has not been performed, in particular because the slow mode is very close (the question of accuracy is evoked in section 5). The second maximum (Figure 7b) seems to belong to the fast magnetosonic mode. The third maximum (Figure 7c) can be identified as an Alfvén wave. One can also notice in Figure 7c that two secondary maxima appear with a lower intensity than the three previous ones. One of these two secondary maxima seems to belong to the slow magnetosonic mode, but the other is located far away from any dispersion relation.

[37] Before pursuing the present wave analyses, it is necessary to emphasize that some caution must be taken when giving names to the identified modes, in order to avoid any possible ambiguity. In fact, although we use names that are familiar in MHD theory, one should keep in mind that the identified waves in high beta and at high frequencies (a few $f_{ci}$) have physical properties which are quite different from those of the MHD modes (more known in small beta plasma). For instance, the Alfvén mode identified previously refers to the so-called "intermediate mode" rather than to the classical shear Alfvén mode. The name "intermediate" is to be taken in the sense that the mode has intermediate phase velocity, i.e., between the phase velocities of the slow and the fast modes. In the same spirit the fast mode in the following refers to the mode with the fastest phase velocity. For this reason we prefer, for the rest of the paper, to put in brackets all these denominations. These denominations are of course to be refined in the future in a frame of a fully kinetic theory.

[38] The identification of all the previous peaks, when based on the only study of the location of their maximum in $\mathbf{k}$ for one given frequency, remains questionable. Two main reasons can challenge it: (1) the spatial aliasing effect, which can make, as explained in section II, a wave appear in the fundamental cell while it really lies outside; and (2) the accuracy of the determination: near the experimental peak of Figure 7a for instance, all the theoretical low frequency modes (except the "fast") are so close together that it is quite difficult to discriminate between them from this only view. The best way of checking the validity of the identifications is to test the continuity of the solutions: it consists in looking at the shape of the peaks in the ($k_x$, $k_y$) plane, but also studying their evolution as functions of $k_z$ and of the frequency. Looking at the $k_z$ planes neighboring the one of Figure 7a confirms for instance that the mode is indeed a mirror mode (not shown).

[39] Now, one may ask whether the neighboring frequencies show the same 3-D distribution of the magnetic energy than the frequency $f_1$? If this is the case, do the previous mode identification remain valid? To answer these questions, we performed the same analysis on three other frequencies $f_2, f_3$, and $f_4$, ranging from $f_1$ to $f_{max}$.

[40] The results corresponding to the frequency $f_2$ are presented in Figure 8. They are similar to the ones obtained for frequency $f_1$: the first maximum (Figure 8a) remains on the mirror mode along the direction $\theta \approx 60°$ whereas the second maximum (Figure 8b) seems to be slightly decoupled from the theoretical dispersion relation of the "fast" mode. The third maximum (Figure 8c) is now out of the

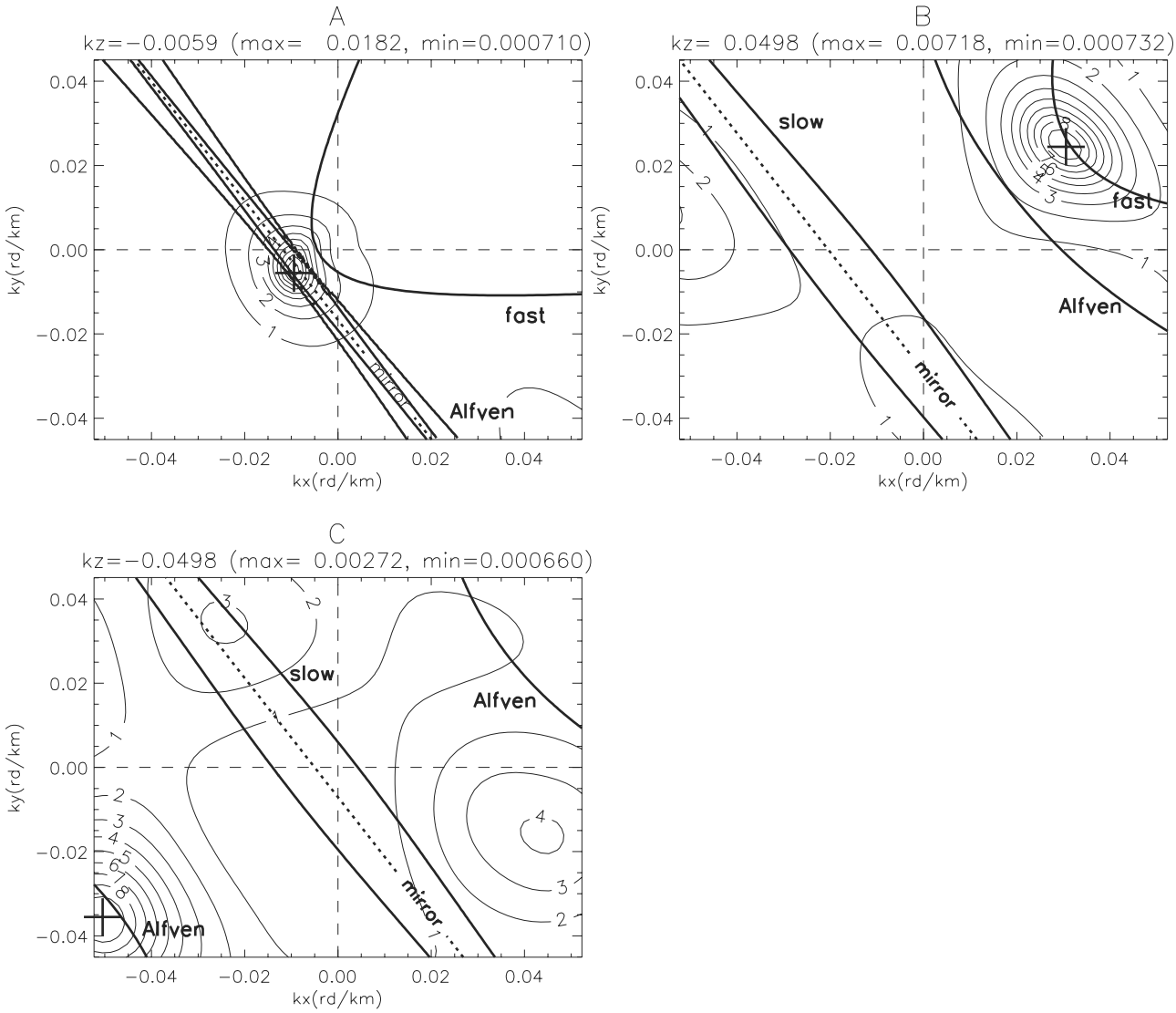


**Figure 7.** For $f_1 = 0.37$ Hz (in the satellite frame), the three $k_z$ planes which contain the three maxima of magnetic energy (labelled by crosses) are displayed. The isocontours are the experimental MFED results, whereas the thick lines are the theoretical dispersion relations. The given "max" and "min" values are the maximum and the minimum energy density [$nT^2/Hz(rd/km)^3$] for the given $k_z$ plane. For the same frequency the magnetic energy is distributed over four wave vectors which appear close to mirror, fast, Alfvén, and slow modes. The peaks in (A, B, C) are ordered from the highest energy to the lowest one.

fundamental cell defined by ($k_{xmax}$, $k_{ymax}$, $k_{zmax}$), which is in a good agreement with the dispersion relation of the Alfvén mode. In Figure 8c, unlike the first secondary maximum which conserves its energy and is still on the slow mode, the second "strange" secondary maximum, identified on $f_1$, seems to have lost the largest part of its energy, reaching thus the level of the noise, as mentioned above. The identification of this weak peak will therefore remain ambiguous.

[41] The results corresponding to the frequency $f_3$ are presented in Figure 9. In Figures 9a and 9b, one can recognize the two first maxima evidenced in the frequencies $f_1$ and $f_2$. The theoretical "fast" mode (Figure 9b) "moves" more away from the peak as the frequency increases. This fact raises some doubt on the identification of this mode as a "fast" mode as it might have been concluded from the only frequency $f_1$. This point is discussed in more detail at the end of this section. Figure 9c shows a new maximum which is close to both the slow and mirror modes, its frequency in the plasma frame is $f = 0.09$ Hz, which may favor the slow mode. In Figure 9d, one can see the extension of the peak previously identified in Figure 9a, besides a new peak (designated by a cross) with a lower intensity. The orientation of the isocontours of energy for this last peak makes its attribution to one of the previous "standard" modes very uncertain. Nevertheless, as reported in Table 1, the corresponding frequency for this peak in the plasma frame is $f_p = 0.67$ Hz ($= 2f_{ci}$), with an angle $\theta \approx 70°$ with respect to $\mathbf{B}_o$. In these conditions, because of the possible resonance with the second gyroharmonic, one may (tentatively) attribute this peak to an ion cyclotron mode, or a "Bernstein-like" mode, in spite it is obviously not electrostatic. There is no way to make this determination less ambiguous since the peak appears in a very narrow frequency band centered on $f_3$ and disappears elsewhere.

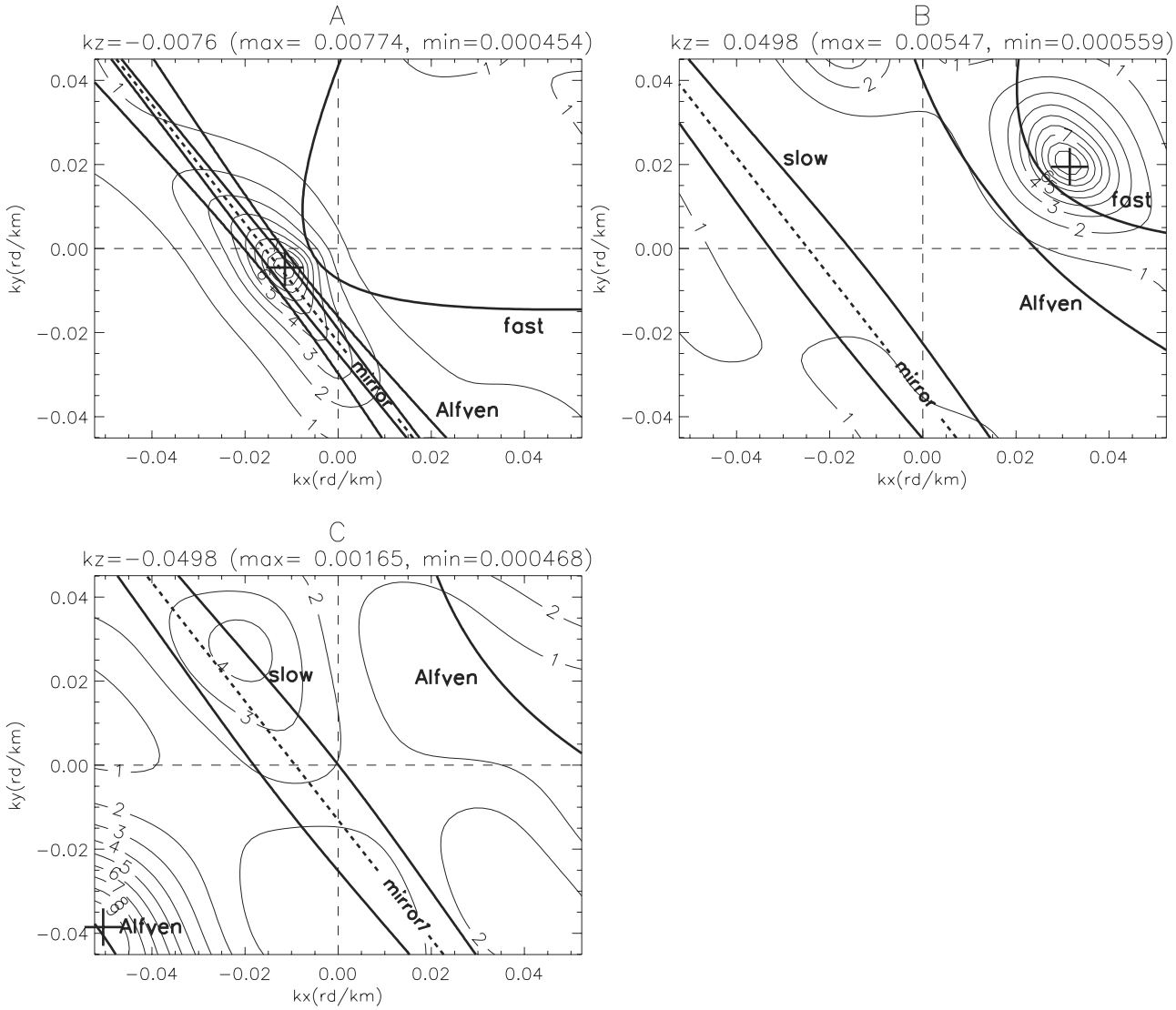


**Figure 8.** Same as Figure 7 for $f_2$ = 0.49 Hz. The main three peaks can be seen at wave vectors close to those identified for $f_1$.

[42] Let us continue with the results associated with frequency $f_4$ (Figure 10): two of the previous maxima identified for frequency $f_3$ are still present (Figures 10a and 10b) with a small variation in the corresponding $k_z$ values. As shown in Figure 10b, the maximum that we have initially identified as a ''fast'' mode is now clearly located far away from the corresponding theoretical dispersion relation. A new maximum area, relatively flat and with a relatively large extension in the ($k_x$, $k_y$) plane can be seen in Figure 10c. It is aligned with the mirror mode. This peak could also be interpreted as the large $k_z$ cut of the same peak already identified as in Figure 10a.

[43] Now we consider in more detail the problem of the suspicious peak identified for all the four frequencies studied here, with a very high level of energy, but without obeying a stable theoretical dispersion relation. Indeed, although, for $f_1$, the peak seems to belong to the ''fast'' mode, the corresponding frequency in the plasma frame is $f_p$ = 1.94 Hz (=5.9 $f_{ci}$), which makes doubtful the existence of a large amount of energy at such high frequencies (apparently not consistent with the view of a turbulent-like power spectrum, decreasing with $k$ and with frequency).

[44] For the four previous studied frequencies the peak has been identified with wave vectors forming a stable angle $\theta \approx 36^\circ$ with respect to $\mathbf{B}_o$. Hence we have compared the theoretical dispersion relation of the ''fast'' mode provided by WHAMP for the given angle $\theta$, to the ''evolution'' of the peak localization in ($\omega$, $\mathbf{k}$) space. In Figure 11 we plotted in ($\omega$, $\mathbf{k}$) domain the location of the experimental peaks, together with the real part of the frequency of the modes determined by WHAMP (except for the mirror mode where $\omega_{mirror}$ = 0 is assumed in the plasma frame). The same comparison is done for the first mirror mode. which forms with $\mathbf{B_0}$ the angle $\theta \approx 61^\circ$ (see Table 1 below). The results of these two comparisons, obtained is the plasma frame, are shown in Figure 11.

[45] So, we can clearly see from Figure 11, that the ''evolution'' of the localization in ($\omega$, $\mathbf{k}$) space of the identified mirror peak is in a good agreement with the theoretical dispersion relation of the mirror mode

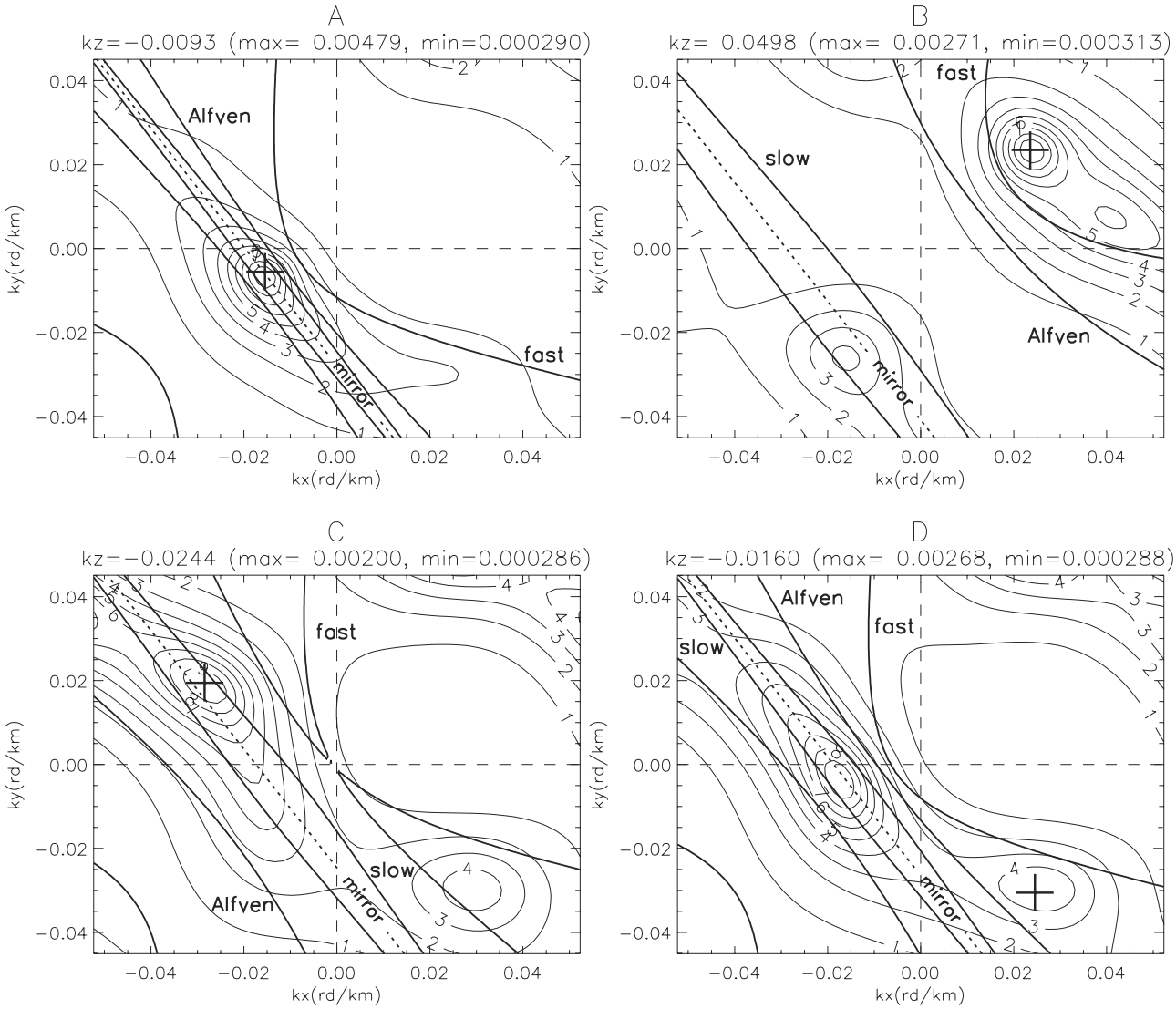


**Figure 9.** Same as Figure 7 for $f_3 = 0.61$ Hz. Besides the two peaks previously identified (panels A, B), two new maxima, symbolized with crosses (panels C and D), appear.

($\omega_{mirror} = 0$). This is not the case concerning the suspicious peak. Indeed, except for $k\rho = 5$ corresponding to the observed frequency $f_1$, the experimental energy maximum does not obey the dispersion relation of the "fast" mode: it exhibits rather a large variation on the modulus of the wave vector with a non significant variation on the frequencies, which is typically characteristic of the mirror mode. Moreover, the orientation of the energy isocontours for this suspicious peak in ($k_x$, $k_y$) plane, as can be seen in the previous figures, appears to be parallel to the mirror mode orientation. So, one may suppose that the wave vector corresponding to this peak may be an alias of an other wave vector in such a way that its frequency in the plasma frame will be zero (mirror mode frequency).

[46] Hence using the formula defined in section 2, which allows us to calculate the reciprocal wave vectors, we check whether one of them makes the experimental peak on the theoretical dispersion relation of an aliased mirror mode. The best candidate is found to have the components: $\Delta k_x = -0.039$ rd/km, $\Delta k_y = -0.029$ rd/km, $\Delta k_z = -0.06$ rd/km.

[47] To materialize this solution, we plot for the previous studied frequencies a new dispersion relation for a reciprocal mirror mode defined as $\omega = (\mathbf{k} + \Delta\mathbf{k}).\mathbf{v}$, where $\Delta\mathbf{k}$ is the reciprocal vector calculated above and $\mathbf{v}$ is plasma velocity vector (Figure 12).

[48] Now, the aliased peak follows exactly the dispersion relation of the reciprocal mirror mode for all the analysed frequencies. This solution is satisfactory enough concerning both the dispersion relation of the mode and the level of the energy, which is now, reported at the expected zero frequency in the plasma frame (Table 1). In this table, negative frequencies correspond to plane waves propagating in a sense opposite to the $\mathbf{k}$ vector.

## 5. Discussion

[49] From the results presented above, some novelties on the ULF magnetic fluctuations can be pointed out. First of all, we have shown that more than one mode can be associated to each given frequency. This result brings very

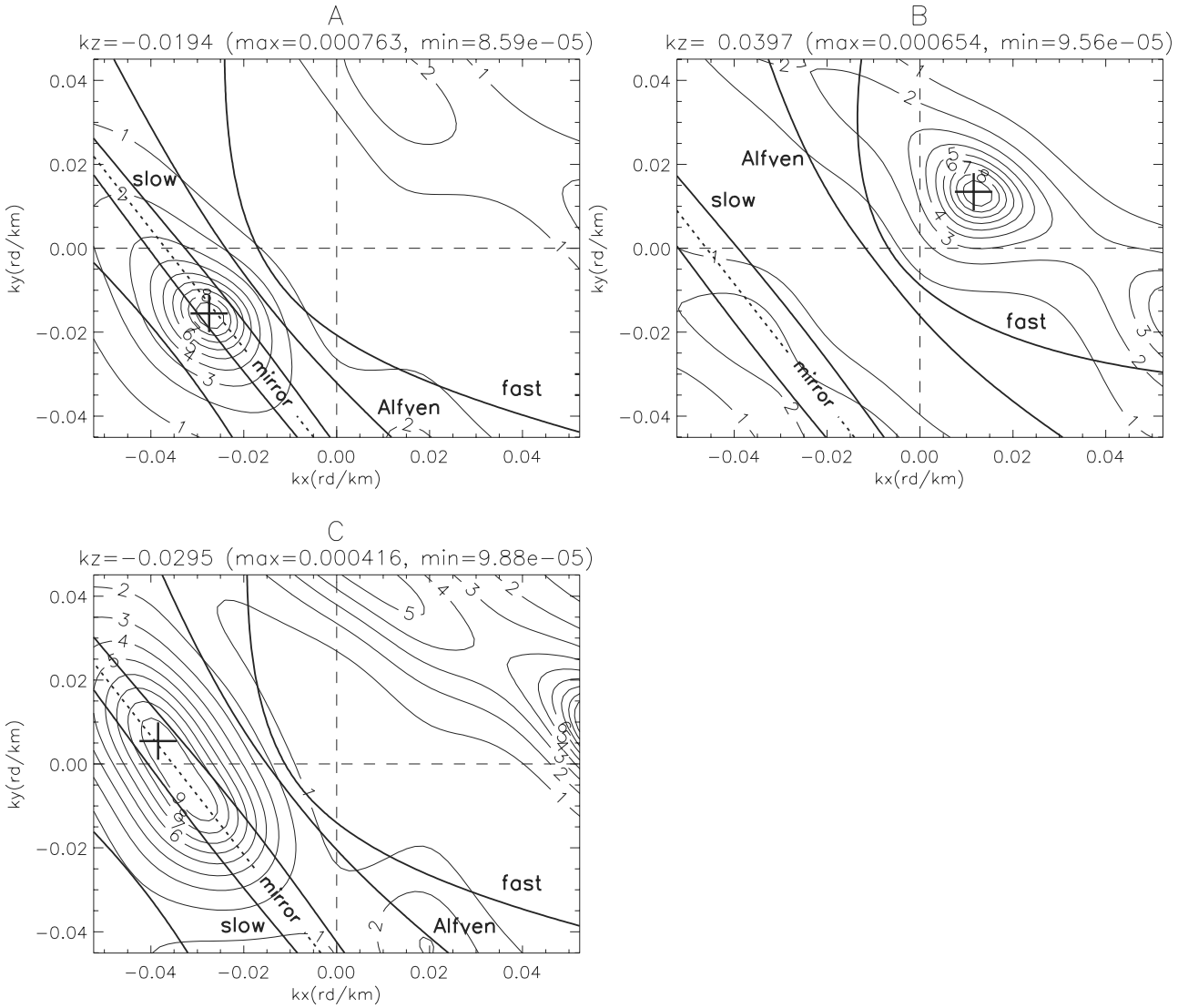


**Figure 10.** Same as Figure 7 for $f_4$ = 1.15 Hz. It shows the same behavior as the frequency $f_3$ for panels A and B, with a new maximum corresponding to mirror mode (panel C).

new and rich information with respect to those presented in previous studies which suggested a rather simple image of the ULF magnetic fluctuations in the magnetosheath by identifying only the dominant longitudinal or transversal component over few hours data. Indeed, by analyzing just a few minutes of data, several different peaks have been identified at once, which seem to belong to mirror, Alfvén, and slow modes. In addition, we observe a few weaker peaks which identification is more ambiguous, like a cyclotron (Bernstein-like) wave. The mirror mode is the dominant wave in the frequency range examined here: mirror waves (zero frequency in the plasma frame) are highly Doppler shifted at frequencies larger than the ion gyrofrequency (in the satellite frame). Their wave vectors form angles ranging from 50° to 70° with respect to the background magnetic field $\mathbf{B}_o$.

[50] Checking whether the existence of the mirror mode can be theoretically explained remains a work to be done. Here, we limited our goal to present a preliminary test of the capability of the k-filtering method for analyzing real experimental data, after it had been applied successfully to simulated data [*Pinçon et al.*, 1994]. However, using WHAMP with the observed parameters or comparing to the literature [*Belmont et al.*, 1992; *Omidi and Winske*, 1995], it is worth noticing that the anisotropy as well as the propagation angles are observed very close to the theoretical values for a local mirror instability at its threshold (considering an anisotropy carried only by bi-Maxwellian ions). Nevertheless, some discrepancies raise from the theoretical modulus of **k** in these conditions: although the modulus $k$ of the first and main peak is of the same order than the theoretical one (within a factor of two), the $k$ of the "aliased mirror" peak (Figure 10) would be about eight times too small. It may raise some suspicion on this last identification, even if such discrepancies can be interpreted, either by refining the distribution model (anisotropy of electrons, non-Maxwellian distributions) or by considering the effects related to nonlinearities or nonhomogeneities (proximity of the magnetopause) [*Omidi and Winske*, 1995]. Let us point however that this peak has an energy 50 times smaller than the main one.

[51] Another imperfection in the previous preliminary identifications may come from the difficulty to really

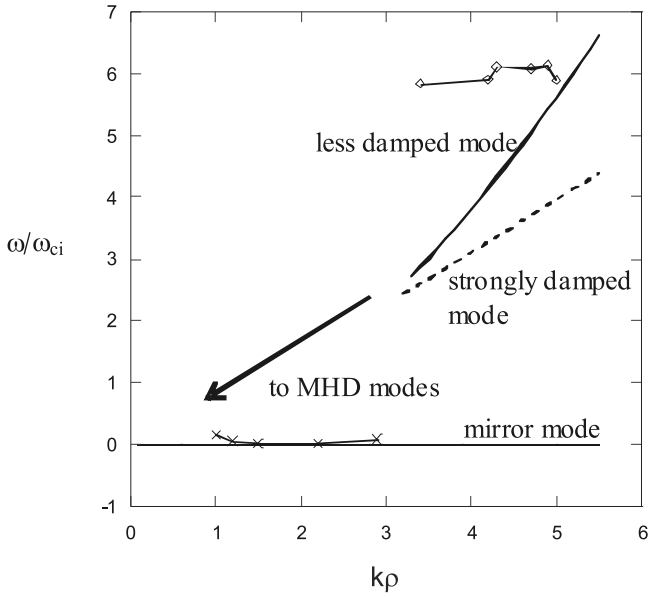


**Figure 11.** The diamonds show the experimental dispersion relation of the aliased peak (propagation angle $\theta \approx 36°$); it is compared with high-frequency theoretical modes for $\theta = 36°$. The crosses show the experimental dispersion relation of the first identified mirror mode (the propagation angle is then $\theta \approx 61°$). Here $\omega_{ci}$ and $\rho$ denote the ion gyrofrequency and the ion Larmor radius, respectively. The observations, when "desaliased," are close to $\omega = 0$, in much better agreement with the theoretical mirror (or slow) mode.

distinguish between the slow and mirror modes, especially for small k (see for instance Figure 1a). The theoretical separation in k-space between some of these modes is probably not much larger than the resolution of the experimental energy distribution.

[52] In addition to the dominant compressive waves, one Alfvén wave has been identified for the frequency $f_1$ which corresponds to a relatively high frequency in the plasma frame $f_p = 2$ Hz. This Alfvén peak, as shown in Figure 8, "leaves out" the box ($k_x$, $k_y$, $k_z$) for frequencies higher than $f_1$; therefore it cannot be studied in more detail as done for the other peaks. Although the energy density of this Alfvén wave is a factor 10 smaller than mirror mode one (Figure 7) and the imaginary part of the solution provided by WHAMP in this case is about of the real part, further analysis, on its polarization for instance, are needed to confirm the Alfvén mode identification at high frequencies.

[53] Two slow waves have been identified for the frequencies $f_1$ and $f_2$ with a lower energy than the other waves, with frequencies in the plasma frame lower than the ion gyrofrequency. They seem to propagate in the same direction ($\theta \approx 40°$) with slightly different frequencies and wavelengths. Let us notice that slow waves may be the dominant compressive waves in the region close to the magnetopause when ion temperature anisotropy and the beta of the plasma do not favor the mirror instabilities (see the references on the slow modes given above). For the frequency $f_3$, besides the possible cyclotron mode evidenced at 2 $f_{ci}$, another slow/mirror mode is also identified, propagating in a direction that forms an angle $\theta \approx 54°$ with $\mathbf{B}_o$. One must keep in mind that contrary to the more usual low beta case, the mode damped by Landau effect in a high beta plasma is the fast mode, which has then a dispersion relation close to $\omega \approx k_{\|} V_{thi}$. The geometrical distribution of the measured wave vectors does not favor any particular direction with respect to the static magnetic field: there is as much energy in the parallel direction than in the perpendicular one. In this case the theoretical assumption, which is sometimes used in analytical studies, that magnetic turbulence would be bidimensional should be taken with a great caution (see, for instance, *Saur et al.* [2002] about magnetic turbulence in the Jovian magnetosphere).

[54] Another point, which illustrates the richness of the results obtained thanks to k-filtering technique, is the 3-D determination of the wave vector of each maximum of energy. Indeed, we can estimate the full Doppler shift on the observed frequency and therefore calculate the corresponding frequency in the plasma frame. Referring to Table 1, we note that waves observed at a one given frequency in the satellite frame with different wave vectors correspond to waves with very different frequencies in the plasma frame. This first estimation of the Doppler effect is of great importance: it seems to have values comparable or even larger than the measured frequency with both positive and negative signs; it alters hence significantly the results and cannot be ignored.

[55] A particular point that can be cleared up, thanks to multipoint measurements and k-filtering results, is the study of wave polarization. Although the fast mode has a right-handed polarization with respect to the local static magnetic field and has been commonly admitted to be the unique mode which can propagate in the magnetosheath above the ion gyrofrequency (at least for a low beta plasma), previous analysis on the magnetic fluctuations in the magnetosheath in the frequency range [1, 10] Hz have proved that this polarization cannot be evidenced [*Rezeau et al.*, 1999]. The present study elucidates this problem: the measured frequency (in the satellite frame) is a superposition of different modes of different natures, with different wave vectors and different frequencies in the plasma frame so that a mixing of polarizations occurs.

[56] We have presented here the raw results as they are provided by the k-filtering technique. One should then wonder what are the different sources of uncertainties that can affect them. Quantifying these uncertainties accurately is a difficult task and it will be postponed to a future work. Nevertheless, we present hereafter the main sources that could affect the results presented above. Some are related to the k-filtering method itself, others to the Cluster II data:

[57] 1. The uncertainty on the MFA frame may affect the comparison with the theoretical modes; we have verified that the parallel directions for each spacecraft differ by less than 5° from the mean parallel direction used.

[58] 2. The accuracy on the four spacecraft positions and the data synchronization: It has been shown that the lack of accuracy in the time synchronisation between the measurements performed on the different spacecraft is a source of errors which may affect seriously the validity of the obtained $P(\omega, \mathbf{k})$ [*Pinçon and Lefeuvre*, 1992]. For a given frequency $\omega$ a time inaccuracy $\delta t$ introduces a phase shift $\phi_t = \omega \delta t$ in the estimation of the power spectra. Phase shifts greater than a few degrees can so distort the $P(\omega, \mathbf{k})$

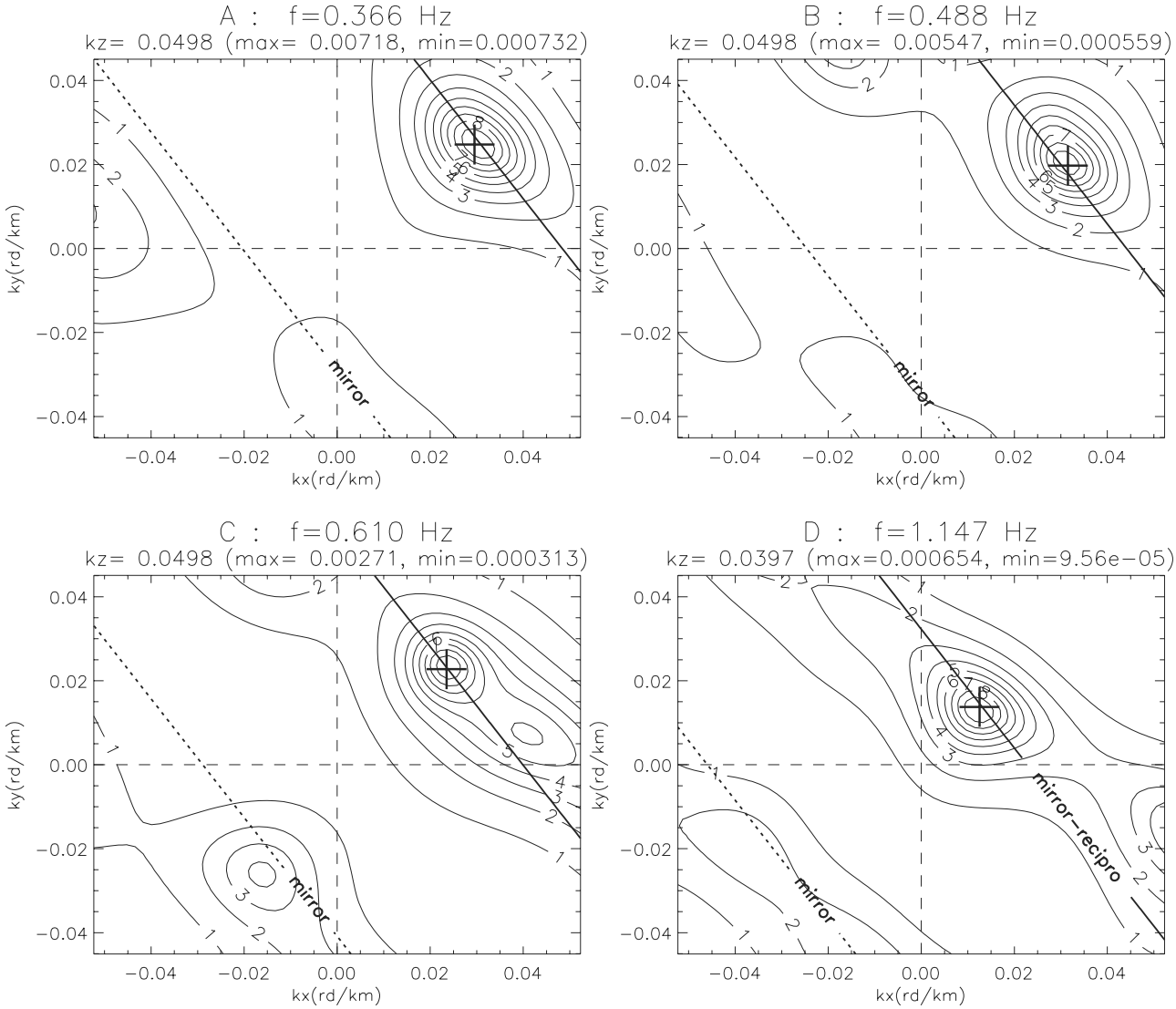


**Figure 12.** The aliased mirror mode (continuous line) is plotted besides the principal one (dashed line) for the four frequencies analyzed above.

estimation. The practical consequence of this is to limit the validity domain of the estimated wave field energy distribution to the low-frequency range. A series of simulations, not shown here, has been performed by *Pinçon and Lefeuvre* [1992] to quantify this effect. It has been shown that for a phase shift below 5°, the errors in $P(\omega, \mathbf{k})$ are hardly noticeable. On board Cluster the magnetic field waveform data are provided with a time accuracy better than 1 ms. Taking into account the fact that all frequencies studied in this paper are below 2 Hz, it comes that the phase shift due to time inaccuracy is always smaller than one degree. Consequently, in the frame of this study, we can safely ignore the errors due to time uncertainty. The effect due to the lack of accuracy in the inter-spacecraft distances is similar to the effect produced by the time synchronisation inaccuracy. For a given wave vector $\mathbf{k}$ in the measured wave field a distance inaccuracy $\delta\mathbf{r}$ introduces a phase shift $\phi_r = \mathbf{k} \cdot \delta\mathbf{r}$ in the estimation of the power spectra. As previously, this effect has been evaluated from simulations. It has been shown that the upper limit of the relative error in the distance has to be fixed between 10% and 20% [*Pinçon and Lefeuvre*, 1992]. For the data used in this study, Cluster satellites are separated by distances of about 100 km. The distances are known with an accuracy better than 5 km which corresponds to a relative error in the inter-spacecraft distance smaller than 5%. Eventually, it appears that for the data presented within this paper, the main source of errors does not come from the phase shifts due to both inaccuracy in time and space but from the noise level in the selected data. As shown by *Pinçon and Lefeuvre* [1991], the smaller is the noise level, the better is the resolving power in $\mathbf{k}$ space. A maximum estimation of the uncertainty in the wave vector localization due to the noise level is given by the half-power width of the peaks evidenced in the $P(\omega, \mathbf{k})$ estimation. An accurate and fully 3-D estimation is a difficult task, however some insight can be carried by looking to the enlargement in the $(k_x, k_y)$ plane for a given $k_z$ value (see for instance Figure 13 and point 3 below).

[59] 3. The uncertainties on the particles data: Concerning the CIS velocity data, which could be suspected to be an important source of uncertainty by Doppler shift of the theoretical dispersion relations, we use in this paper the

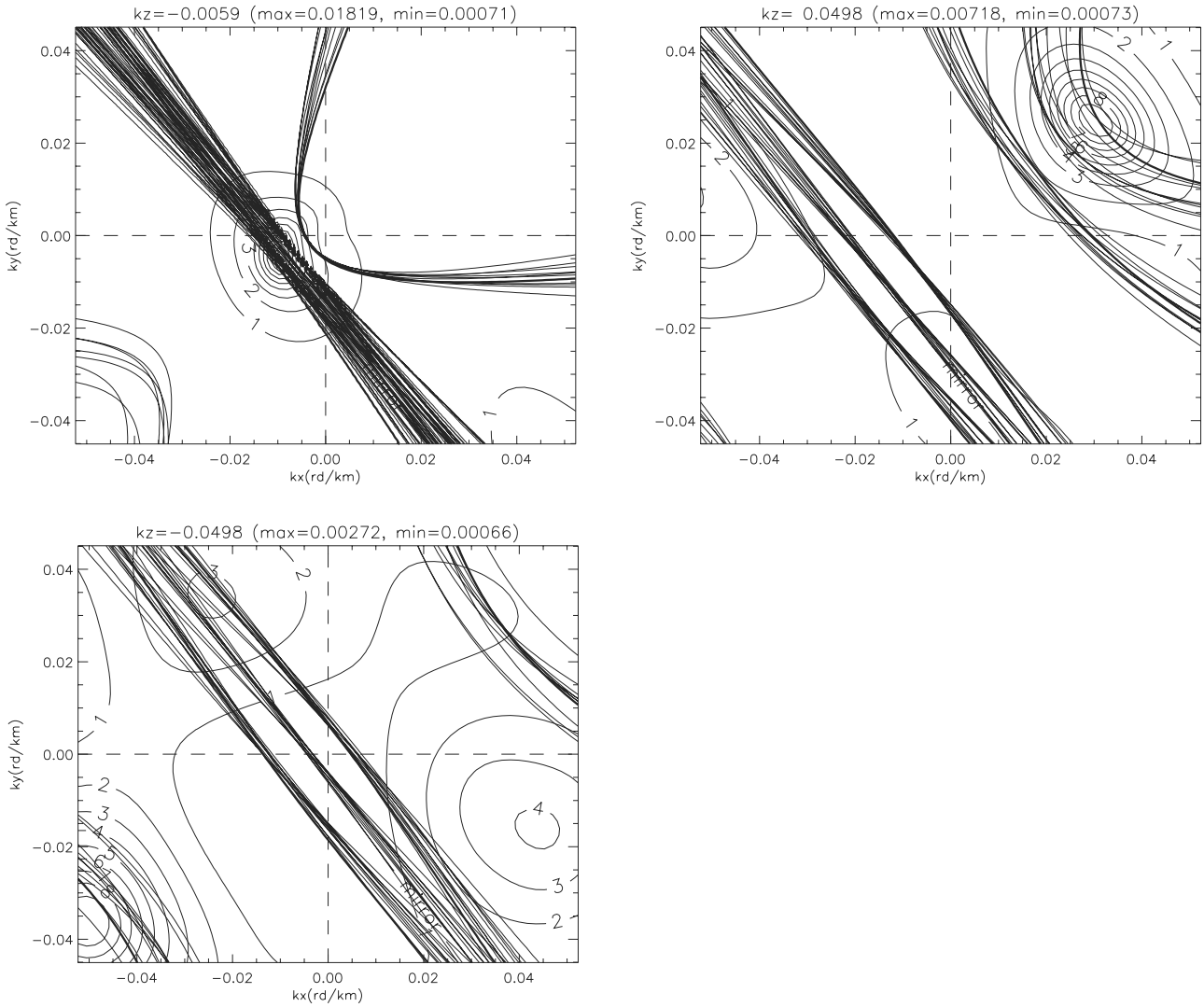


**Figure 13.** Same as Figure 7, except that the theoretical dispersion relations are plotted for the frequency $f_1$ by varying randomly the plasma velocities in the interval $v_i \pm \delta v_i$ where $\delta v_i/v_i = 20\%(i = x, y, z)$, thus giving a network of thin lines. Unlike for the slow and the mirror modes that seem to be indiscernible especially for small k (top-left panel), the other modes are well separated in the k-space.

most accurate determinations provided by the CIS2 instrument that have the best resolution in velocity space. Calibrations before flight, simulations of onboard moment calculations, and interspacecraft comparisons (see Figure 5) allow asserting that ion velocity components are determined with an accuracy of 5% or even less for a magnetosheath plasma. In order to quantify this error source in the accuracy of the result, we plotted in Figure 13 the dopplerized theoretical dispersion relations for velocity components varying randomly in the volume bounded by $[v_i \pm \delta v_i]$, where $\delta v_i/v_i = 20\%$ $(i = x, y, z)$, i.e., in a volume much larger than the presently accepted CIS errors. This overestimated and improbable error, on the CIS data alone, is used in order to take into account, indirectly, the error on the wave vectors determination that could lead to some enlargement of the identified peaks, as it was mentioned above. With the given maximum uncertainties it appears difficult to really distinguish, for the main peak, between the main mirror and slow modes. On the contrary, the other theoretical modes are well organized in "bands" with a width in **k**-space smaller than the separation of the identified peaks or between themselves.

[60] Other minor sources of errors can be cited such as the temperature and density uncertainties on the calculation of the theoretical modes. However, they seem to have a contribution much smaller (even negligible) then those studied above. Although this study of the effect of the different sources of uncertainties is not yet complete, the evident quality of the results obtained seems to indicate that the combination of all these uncertainties remain of limited importance.

[61] One of the improvements envisaged for the future is to include the electric field in the k-filtering analysis, together with the corresponding new Maxwell constraints. This will allow to bring more information on the electrostatic part of the waves, which will certainly improve our global view on the magnetic fluctuations. This work is in progress.

## 6. Conclusions

[62] The present study is one of the first attempts to disentangle temporal and spatial variations characterizing the magnetic fluctuations in the magnetosheath thanks to Cluster II data. Applying k-filtering technique to a combination of four point measurement data from Cluster II, we have determined a 3-D magnetic wave field energy distribution for four frequencies chosen in the frequency range [0.35, 1.4] Hz. For each frequency the energy appears to be expanded over more than one wave vector. We have checked whether the distribution of the maxima of energy in wave vector domain obeys the dispersion relations of the ULF modes. Therefore we have compared these experimental results to a simple model of low frequency linear waves. Besides the mirror mode, which is confirmed to be dominant even at observed high (nonzero) frequencies, Alfvén and slow modes can also be identified. The imaginary parts of the theoretical solution provided by WHAMP are nonzero. Hence one may suggest that weak nonlinear interaction between low frequency modes may work to overcome the linear kinetic damping. Indeed, several experimental arguments may be advanced to justify a model of weak turbulence for studying coupling between large and small scales magnetosheath fluctuations: (1) the weak level of the magnetic fluctuations compared to the background magnetic field $B_o$ (less than 15%, Figure 2), (2) the decomposition of the magnetosheath magnetic energy over eigenmodes close to the ULF modes (mirror, Alvfen/intermediate, slow), (3) the shape of the magnetic power spectrum describing the cascade of energy from large to small scales (Figure 3).

[63] One other interesting result is the estimation of the Doppler shift on the observed frequencies. The corresponding energy appears to be due to a superposition of different plane waves in the plasma frame. This explains why analysis on the waves polarization fails when Doppler shift is ignored.

[64] The results presented above on the wave identification will have to be confirmed and completed in a more refined study, in particular, on the polarization associated with the different maxima. A problem that will be solved in the near future is the possibility to infer the spatial spectrum of the fluctuations from the temporal one: $B^2(\omega, \mathbf{k}) \rightarrow \tilde{B}^2(\mathbf{k})$ by integrating over the whole studied frequency range. This point is of great usefulness for all space plasma turbulence theories based on deriving the power spectrum of the turbulent field and calculating its slope, which characterizes the large-to-small scales coupling. This problem could not be "solved" hitherto without strong assumptions like the Taylor frozen-in assumption $\omega \approx$ kV (adopted, for instance, in the solar wind studies, where the Doppler shift is indeed dominant) or the hypothesis of one unique wave with a known dispersion. If, in a high-plasma beta, the whole spectrum of the fluctuations is confirmed to be dominated by Doppler shifted mirror modes, one may hence use the familiar Taylor assumption to calculate roughly the slope of the spatial spectrum from the temporal one. Otherwise, we think that inferring the slope of the magnetic fluctuations spectrum in **k** space from the one in $\omega$ space requires, first, to apply k-filtering technique to a large number of frequencies; the spatial distribution of the calculated wave vectors is a key information in determining the actual slope of the spatial spectrum. This is related to the familiar questions in turbulence theories whether the turbulence is isotropic or bidimensional. Indeed, if the obtained wave vectors are directed in a particular direction, for instance the perpendicular one with respect to the static magnetic field, we will be able to deduce the slope of the frequency-integrated spectrum in **k** space only along the given direction: $B^2(\omega, \mathbf{k}) \rightarrow \tilde{B}^2(\mathbf{k}) \approx f(k_{\|}) k_{\perp}^{-\lambda}$. Nevertheless, as it has been shown above (and this may be generally the case in high beta plasma), the spatial distribution of wave vectors confirms that they can be oriented along the static magnetic field as well as in perpendicular direction. In this case, one may check in more detail the validity of a possible isotropic assumption.

[65] To answer these questions, the previous experimental results should be confirmed for a wide frequency range, even for frequencies below the ion gyrofrequency. Moreover, in order a construct a global view on the magnetic fluctuations in the magnetosheath, similar studies are needed in the case of low beta magnetosheath plasma, where we expect that other waves than the mirror mode may be dominant.

[66] The questions concerning the accuracy attained by the method have been briefly discussed in section 5. We think that it is however important to mention the relative stability of the results: the same analysis has been repeated on a time interval 25 minutes later (around 0600) where the spacecraft remained in the magnetosheath. We find almost all the previous results on the wave identification, and the main conclusions mentioned above remain valid.

[67] The richness in information allowed by the k-filtering technique at once on the 3-D waves recognition, dispatching of energy over these waves and estimation of the Doppler effect offers new opportunities to explore new aspects of the magnetosheath physics, and can be extended to a large part of plasma space contexts. It will certainly allow also many advances in different contexts, for instance for checking separately the temporal and spatial resonance conditions in the case of coupling of quasi-monochromatic waves, as demonstrated on the numerical simulation by *Pinçon et al.* [1994].

[68] **Acknowledgments.** Shadia Rifai Habbal thanks both referees for their assistance in evaluating this paper.

## References

Anderson, B. J., and S. A. Fuselier, Magnetic pulsation from 0.1 to 4 Hz and associated plasma properties in the Earth's subsolar magnetosheath and plasma depletion layer, *J. Geophys. Res.*, *98*, 1461–1479, 1993.

Anderson, B. J., S. A. Fuselier, S. P. Gary, and R. E. Denton, Magnetic spectral signatures in the Earth's magnetosheath and plasma depletion layer, *J. Geophys. Res.*, *99*, 5877–5891, 1994.

Balikhin, M. A., T. Dudok de Wit, H. S. K. Alleyne, L. J. C. Woolliscroft, S. N. Walker, V. Krasnosel'skikh, W. A. C. Mier-Jedrzejeowicz, and W. Baumjohann, Experimental determination of the dispersion of waves observed upstream of a quasi-perpendicular shock, *Geophys. Res. Lett.*, *24*, 787–790, 1997.

Balikhin, M. A., S. Schwartz, S. N. Walker, H. S. K. Alleyne, M. Dunlop, and H. Lühr, Dual-spacecraft observation of standing waves in the magnetosheath, *J. Geophys. Res.*, *106*, 25,395–25,408, 2001.

Balogh, A., et al., The Cluster magnetic field investigation, *Space Sci. Rev.*, *79*, 65–91, 1997.

Bates, I., M. Balikhin, H. Alleyne, and M. Andre, Minimum-variance free determination of magnetosheath wave propagation vectors, in *Les Woolliscroft Memorial Conference Sheffield Space Plasma Meeting: Multipoint Measurements Versus Theory, ESA SP-492*, pp. 133, Eur. Space Agency, Paris, 2001.

Belmont, G., and L. Rezeau, Magnetopause reconnection induced by magnetosheath Hall-MHD fluctuations, *J. Geophys. Res.*, *106*, 10,751–10,760, 2001.

Belmont, G., D. Hubert, C. Lacombe, and F. Pantellini, Mirror mode and other compressive ULF modes, in *Proceedings of the 26th ESLAB Symposium: Study of the Solar-Terrestrial System, ESA SP-346*, Eur. Space Agency, Paris, 1992.

Capon, J., High-resolution frequency-wavenumber spectrum analysis, *Proc. IEEE*, *57*, 1408–1418, 1969.

Chanteur, G., Spatial interpolation for four spacecraft: Theory, in *Analysis Methods for Multi-Spacecraft Data*, *Sci. Rep.*, pp. 349–369, Int. Space Sci. Inst., Bern, Switzerland, 1998.

Cornilleau-Wehrlin, N., et al., The Cluster Spatio-Temporal Analysis of Field Fluctuations (STAFF) Experiment, *Space Sci. Rev.*, *79*, 107–136, 1997.

Décréau, P. M. E., et al., WHISPER, A resonance sounder and wave analyser: Performances and perspectives for the cluster mission, *Space Sci. Rev.*, *79*, 157–193, 1997.

Denton, R. E., S. P. Gary, B. J. Anderson, S. A. Fuselier, and M. K. Hudson, Low frequency magnetic spectra in the magnetosheath and plasma depletion layer, *J. Geophys. Res.*, *99*, 5893–5901, 1994.

Denton, R. E., S. P. Gary, B. J. Anderson, S. A. Fuselier, and M. K. Hudson, Low frequency magnetic fluctuation spectra in the magnetosheath and plasma depletion layer, *Geophys. Res.*, *100*, 5665–5679, 1995.

Dudok de Wit, T., V. V. Krasnosel'skikh, S. D. Bale, M. W. Dunlop, H. Lühr, S. J. Schwartz, and L. J. C. Woolliscroft, Determination of dispersion relations in quasi-stationary plasma turbulence using dual satellite data, *Geophys. Res. Lett.*, *22*, 2653–2656, 1995.

Gary, S. P., B. J. Anderson, R. E. Denton, S. A. Fuselier, M. E. McKean, and D. Winske, Ion anisotropies in the magnetosheath, *Geophys. Res. Lett.*, *20*, 1767–1770, 1993.

Gleaves, D. G., and D. J. Southwood, Magnetohydrodynamic fluctuations in the Earth's magnetosheath at 1500 LT: ISEE 1 and ISEE 2, *J. Geophys. Res.*, *96*, 129–142, 1991.

Hubert, D., Nature and origin of wave modes in the dayside Earth's magnetosheath, *Adv. Space Res.*, *14*, 755–764, 1994.

Hubert, D., C. Lacombe, C. C. Harvey, and M. Moncuquet, Nature, properties and origin of low-frequency waves from an oblic shock to the inner magnetosheath, *J. Geophys. Res.*, *103*, 26,783–26,798, 1998.

Lacombe, C., F. G. E. Pantellini, D. Hubert, C. C. Harvey, A. Mangeney, G. Belmont, C. T. Russell, and J. T. Gosling, Mirror and alfvenic waves observed by ISEE 1–2 during crossing of the Earth's bow shock, *Ann. Geophys.*, *10*, 772–784, 1992.

Lacombe, C., G. Belmont, D. Hubert, C. C. Harvey, A. Mangeney, C. T. Russell, J. T. Gosling, and S. A. Fuselier, Density and magnetic filed fluctuations observed by ISEE 1–2 in the quiet magnetosheath, *Ann. Geophys.*, *13*, 343–357, 1995.

Lucek, E. A., M. W. Dunlop, A. Balogh, P. Cargill, W. Baumjohann, E. Georgescu, G. Haerendel, and K. H. Fornacon, Identification of magnetosheath mirror modes in Equator-S magnetic field data, *Ann. Geophys.*, *17*, 1560–1573, 1999.

Luhmann, J. G., C. T. Russel, and R. C. Elphic, Spatial distribution of magnetic field fluctuations in the dayside magnetosheath, *J. Geophys. Res.*, *91*, 1711–1715, 1986.

Neubauer, F. M., and K. H. Glassmeier, Use of an array of satellite as a wave telescope, *J. Geophys. Res.*, *95*, 19,115–19,122, 1990.

Omidi, N., and D. Winske, Structure of the magnetopause inferred from one-dimensional hybrid simulations, *J. Geophys. Res.*, *100*, 11,935–11,955, 1995.

Omidi, N., A. O'Farrell, and D. Krauss-Verban, Sources of magnetosheath waves and turbulence, *Adv. Space Res.*, *14*, 745–754, 1994.

Pinçon, J. L., and F. Lefeuvre, Local characterization of homogeneous turbulence in a space plasma from simultaneous measurements of field components at several points in space, *J. Geophys. Res*, *96*, 1789–1802, 1991.

Pinçon, J. L., and F. Lefeuvre, The application of the generalized Capon method to the analysis of a turbulent field in space plasma: Experimental constraints, *J. Atmos. Terr. Phys.*, *54*, 1237–1247, 1992.

Pinçon, J. L., and U. Motschmann, Multi-spacecraft filtering: General framework, in *Analysis Methods for Multi-Spacecraft Data*, edited by G. Paschmann and P. W. Daly, pp. 65–78, Int. Space Sci. Inst., Bern, Switzerland, 1998.

Pinçon, J. L., F. Lefeuvre, and G. Chanteur, Multipoint analysis of a simulated bi-dimensional MHD turbulence: Application to the CLUSTER mission, in *Solar-Terrestrial Energy Program: Initial Results From STEP Facilities and Theory Campaign*, *COSPAR Colloquia Ser.*, vol. 5, edited by D. N. Baker, V. O. Papitashvili, and M. J. Teague, pp. 785–790, Pergamon, New York, 1994.

Rème, H., et al., The Cluster Ion Spectrometry (CIS) Experiment, *Space Sci. Rev.*, *79*, 303–350, 1997.

Rezeau, L., G. Belmont, C. Briand, N. Cornilleau-Wehrlin, and F. Reberac, Spectral law and polarization properties of the low frequency waves at the magnetopause, *Geophys. Res. Lett.*, *26*, 651–654, 1999.

Rezeau, L., et al., A case study of low frequency waves at the magnetopause, *Ann. Geophys.*, *19*, 1463–1470, 2001.

Robert, P., A. Roux, C. C. Harvey, M. W. Dunlop, P. W. Daly, and K. H. Glassmeier, Tetrahedron geometric factors, in *Analysis Methods for Multi-Spacecraft Data*, *Sci. Rep.*, pp. 323–348, Int. Space Sci. Inst., Bern, Switzerland, 1998.

Rönnmark, K., *Report 179*, Kiruna Geophys. Inst., Kiruna, Sweden, 1982.

Saur, J., H. Politano, A. Pouquet, and W. H. Matthaeus, Evidence for weak MHD turbulence in the middle magnetosphere of Jupiter, *Astron. Astrophys.*, *386*, 699–708, 2002.

Song, P., C. T. Russell, and M. F. Thomsen, Waves in the inner magnetosheath: A case study, *J. Geophys. Lett.*, *19*, 2191–2194, 1992.

Song, P., C. T. Russell, and S. P. Gary, Identification of low-frequency fluctuations in the terrestrial magnetosheath, *J. Geophys. Res.*, *99*, 6011–6025, 1994.

A. Balogh, Space and Atmospheric Group, Blackett Laboratory, Imperial College, Prince Consort Road, London, SW7 2BZ, UK. (a.balogh@ic.ac.uk)

G. Belmont, P. Canu, G. Chanteur, N. Cornilleau-Wehrlin, L. Mellul, L. Rezeau, P. Robert, and F. Sahraoui, Centre d'Etude des Environnements Terrestre et Planétaires/Centre National de la Recherche Scientifique-Université de Versailles Saint Quentin En Yvelines, 10-12 avenue de l'Europe, 78140 Vélizy, France. (gerard.belmont@cetp.ipsl.fr; partick.canu@cept.ipsl.fr; gerard.chanteur@cetp.ipsl.fr; nicole.cornilleau@cetp. psl.fr; lidia.mellul@cetp.ipsl.fr; laurence.rezeau@cetp.ipsl.fr; patrick.robert@cetp.ipsl.fr; fouad.sahraoui@cetp.ipsl.fr)

J. M. Bosqued, Centre d'Etude Spatiale des Rayonnements, 9 avenue du colonel Roche, 31028 Toulouse cedex 4, France. (bosqued@cesr.fr)

J. L. Pinçon, Laboratoire de Physique et Chemie de l'Environnement, 3A avenue de la Recherche Scientifique, 45071 Orleans Cedex 2, France. (jlpincon@cnrs-orleans.fr)

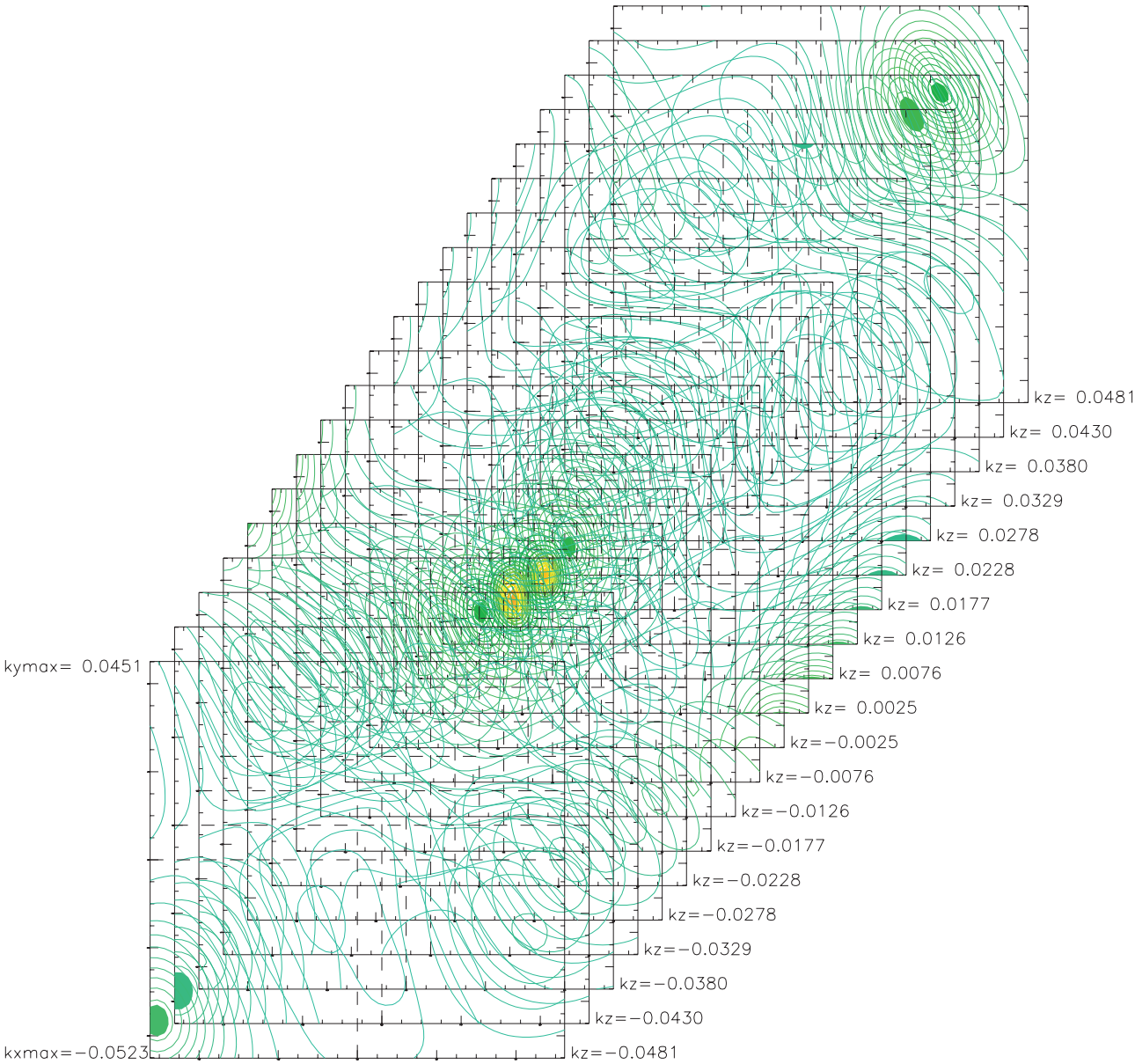


**Figure 6.** Three-dimensional display of the MFED in ($k_x$, $k_y$, $k_z$) space for the frequency $f_1$ = 0.37 Hz. Energy isocontours are drawn in ($k_x$, $k_y$) planes for 20 values of $k_z$ . $k_x$ and $k_y$ values belong respectively to [−0.0523,0.0523] rd/km and to [0.045,0.0451] rd/km. Filled regions represent the three significant maxima. The colour scale goes from black to white with decreasing energy (or from red to blue on the color plate).